

Structural reliability applications of non-stationary spectral characteristics

Michele Barbato¹, A.M.ASCE, and Joel P. Conte², M.ASCE.

ABSTRACT

This paper presents new closed-form analytical approximations to the first-passage problem in structural reliability by using the exact closed-form solutions for the spectral characteristics of non-stationary random processes. The first-passage problem applied to a structural system possibly with random parameters and subjected to stochastic loading consists in computing the probability of a response quantity exceeding a deterministic threshold in a given exposure time. This paper also investigates, based on benchmark problems, the absolute and relative accuracy of analytical approximations of the time-variant failure probability, such as Poisson, classical Vanmarcke and modified Vanmarcke approximations, in the case of non-stationary random vibration. The classical and modified Vanmarcke approximations are expressed as time integrals of the closed-forms of the corresponding hazard functions. These closed-forms refer to linear elastic systems subjected to stationary and non-stationary base excitation from at rest initial conditions, and are obtained using recently developed exact closed-form solutions for the time-variant bandwidth parameter. These closed-form Vanmarcke's approximate solutions to the first-passage problem are compared to the well known Poisson approximation and accurate simulation results obtained via the Importance Sampling using Elementary Events (ISEE) method for two benchmark applications: (1) a set of linear elastic SDOF systems defined by different natural periods and damping ratios, and (2) an idealized yet realistic three-dimensional asymmetric steel building model. The linear elastic SDOF systems are subjected to white noise base excitation from at rest initial conditions, while the steel building model is subjected, from at rest initial conditions, first to white noise and then to a time-modulated colored noise base excitation. The retrofit of this second benchmark structure with viscous dampers is also considered, allowing (1) to illustrate the use of the newly available closed-form approximations of the failure probability for non-classically damped linear elastic systems,

¹ Assistant Professor, Department of Civil & Environmental Engineering, Louisiana State University and A&M College, 3531 Patrick F. Taylor Hall, Nicholson Extension, Baton Rouge, Louisiana 70803, USA; E-mail: mbarbato@lsu.edu

² Professor, Department of Structural Engineering, University of California at San Diego, 9500 Gilman Drive, La Jolla, California 92093-0085, USA; E-mail: jpconte@ucsd.edu (corresponding author)

and (2) to show an example of practical use in structural engineering of the presented analytical solutions. The results presented in this study show that, for non-stationary random vibration problems, the two Vanmarcke approximations can improve considerably the estimates of the time-variant failure probability for the first-passage problem when compared to the simpler Poisson approximation.

CE DATABASE SUBJECT HEADINGS: Stochastic processes; time-variant failure probability; spectral moments; non-classically damped MDOF systems; Monte Carlo simulation; importance sampling using elementary events.

Accepted Manuscript
Not Copyedited

INTRODUCTION

In many engineering fields, the importance of using stochastic processes to model dynamic loads such as earthquake ground motions and wind action on civil structures, ocean wave induced forces on ships and offshore structures, effects of road/track surface roughness on automotive structures, and atmospheric turbulence on aerospace structures has been widely recognized. Extensive research has been devoted to the development of analytical methods and numerical simulation techniques related to modeling of stochastic loads and analysis of their effects on structures (Lin 1976; Priestley 1987; Lutes and Sarkani 2004). These effects are stochastic in nature and, in general, are represented by random processes which are non-stationary in both amplitude and frequency content (Yeh and Wen 1990; Papadimitriou 1990; Conte 1992). Modern design codes consider loading uncertainty as well as parameter and modeling uncertainties to ensure satisfactory designs. Methodologies for time-variant reliability analysis have gained significant importance, as they provide a sound analytical basis for evaluating probabilistically the satisfaction of prescribed structural performance criteria, e.g., in the context of the emerging Performance-Based Earthquake Engineering (PBEE) methodology (Cornell and Krawinkler 2000; Moehle and Deierlein 2004) and the new generation of seismic design codes inspired by the PBEE methodology (AASHTO 1998; ICC 2003; BSSC 2004; ATC-58 2005).

The probability of failure over a given interval of time (i.e., probability of a response vector process outcrossing a general limit-state surface during an exposure time) is the fundamental result sought in a time-variant reliability analysis. For a large class of structural applications, the failure condition can be identified as the exceedance of a scalar deterministic threshold by a linear combination of scalar response quantities. To date, no exact closed-form solution of this problem (referred to in the literature as the first-passage problem) is available, even for the simplest case of structural model (deterministic linear elastic SDOF system) subjected to the simplest stochastic load model (stationary Gaussian white noise). The Monte Carlo simulation technique is the only general method accommodating for non-stationarity and non-Gaussianity of the excitation as well as nonlinearity in the structural behavior and

uncertainty/randomness in the structural parameters. However, it is computationally extremely expensive if not impossible. Nevertheless, an analytical upper bound of the time-variant probability of failure can be readily obtained when the mean out-crossing rates of the response quantities of interest are available (Lin 1976). Several direct approximations of this failure probability also exist that make use of various statistics of the response quantities of interest (Crandall 1970; Wen 1987). In particular, Poisson and Vanmarcke approximations offer a good compromise between accuracy and computational effort (Rice 1944, 1945; Corotis et al. 1972). Vanmarcke suggested two different approximations (Vanmarcke 1975), called classical and modified Vanmarcke approximation, respectively, which both require the computation of the bandwidth parameter of the considered stochastic process, in addition to the other stochastic moments required for computing the mean out-crossing rate and Poisson approximation. The two Vanmarcke approximations were first derived for stationary problems (stationary Vanmarcke approximations), and then extended to non-stationary problems (non-stationary Vanmarcke approximations) (Corotis et al. 1972; Vanmarcke 1975). More recent work by Di Paola (1985) and Michaelov et al. (1999a,b) provided new insight into the non-stationary spectral characteristics required by the non-stationary Vanmarcke approximations, suggesting a more appropriate definition of the bandwidth parameter for real-valued non-stationary random processes. In previous work (Barbato and Conte 2008), the authors extended these last results to the computation of stochastic characteristics of complex-valued non-stationary random processes and used such extension for finding the exact closed-form solution of the time-variant bandwidth parameter for the classical problem of SDOF and MDOF linear elastic systems subjected to white noise excitation from at rest initial conditions. In Barbato and Vasta (2010), the closed-form solution of the time-variant bandwidth parameter was found for classically and non-classically damped MDOF linear elastic systems subjected to time-modulated colored noise excitation.

This paper focuses on closed-form analytical approximations to the first-passage problem in structural reliability. After defining the problem, existing analytical approximations are briefly reviewed. Then, the exact closed-forms for the spectral characteristics of non-stationary random processes, recently derived by

the authors, are used to define integral representations of such analytical approximations of the time-variant failure probability, namely Poisson, classical Vanmarcke and modified Vanmarcke approximations. Finally, two sets of benchmark models, consisting of a set of linear elastic SDOF systems with different natural periods and damping ratios and a realistic three-dimensional asymmetric three-story building model, are used to compare these analytical approximations with accurate simulation results obtained through the Importance Sampling using Elementary Events (ISEE) method (Au and Beck 2001a). The absolute and relative accuracy of the considered closed-form approximations to the time-variant failure probability, obtained at a very small fraction of the computational cost of the ISEE results, is carefully investigated for a wide range of values of the failure probability. To the authors' knowledge, this paper presents the first rigorous appraisal of the accuracy of the two Vanmarcke approximations of the time-variant failure probability for the first-passage reliability problem in the context of non-stationary random vibration.

It is noteworthy that structural reliability analysis of nonlinear (deterministic or uncertain) dynamic systems is a very active area of research. In fact, several methodologies have been recently developed to numerically estimate the time-variant failure probability relative to the first-passage problem for nonlinear dynamic models of structures, e.g., the subset simulation method (Au and Beck 2001b; Ching et al. 2005a,b; Katafygiotis and Cheung 2005), the tail equivalent linearization method (Fujimura and Der Kiureghian 2007), the path integration method (Naess and Moe 2000), advanced/enhanced Monte Carlo simulation-based methods (Pradlwarter and Schueller 2004, Pradlwarter et al. 2007, Naess et al. 2009), and the hybrid Design Point - Response Surface - Simulation method (Barbato et al. 2008). Analytical solutions for the time-variant failure probability, such as the ones presented in this paper for the case of linear elastic systems subjected to Gaussian non-stationary excitations, are extremely useful for validation, in the linear range, of both existing and new numerical methods for time-variant structural reliability analysis.

FIRST-PASSAGE PROBLEM IN STRUCTURAL RELIABILITY

In the present study, the time-variant probability of failure of a dynamic structural system is defined as the probability that a quantity (linearly) related to the displacement and velocity responses (e.g., absolute displacement, relative displacement, elastic force) of the system exceeds a given (deterministic and time invariant) threshold ζ . The problem of evaluating this time-variant probability of failure is also known as first-passage problem and has been presented in the literature as single-barrier problem (random process up-crossing or down-crossing a given threshold) or as double-barrier problem (absolute value of the random process exceeding a given threshold).

An analytical upper-bound of the time-variant probability of failure, $P_{f,x}(\zeta^+, t)$, is obtained by integrating in time the mean up-crossing rate, $\nu_x(\zeta^+, t)$, of the considered process, $X(t)$, corresponding to the fixed deterministic threshold ζ^+ (single-barrier problem), as

$$P_{f,x}(\zeta^+, t) = \sum_{n=1}^{\infty} P[N(t)=n] \leq \sum_{n=1}^{\infty} n \cdot P[N(t)=n] = E[N(t)] = \int_0^t \nu_x(\zeta^+, \tau) d\tau \quad (1)$$

where $E[\dots]$ = expectation operator, and $N(t)$ = number of up-crossings up to time t . The mean up-crossing rate $\nu_x(\zeta^+, t)$ can be obtained from the well known Rice formula (Rice 1944, 1945), for which a closed-form solution is available in the case of Gaussian processes (Lutes and Sarkani 2004). In general, a numerical estimate of $\nu_x(\zeta^+, t)$ can be obtained through the limiting formula proposed by Hagen and Tvedt (1991). The time-variant failure probability $P_{f,x}(\zeta^+, t)$ is commonly expressed in the following functional form

$$P_{f,x}(\zeta^+, t) = 1 - P[X(t=0) < \zeta^+] \cdot \exp\left\{-\int_0^t h_x(\zeta^+, \tau) d\tau\right\} \quad (2)$$

where $P[X(t=0) < \zeta^+] =$ probability that, at time $t=0$, the random process $X(t)$ is below the failure threshold ζ^+ (i.e., probability that the system is safe at time $t=0$) and $h_x(\zeta^+, t) =$ time-variant hazard function defined such that $\int_0^t h_x(\zeta^+, \tau) d\tau =$ probability of an up-crossing of level ζ^+ during the time interval

$[t, t+dt]$ given no up-crossing up to time τ (i.e., probability of first up-crossing event in time interval $[t, t+dt]$). For at rest initial conditions, $P[X(t=0) < \zeta^+] = 1$. Up to date, only approximate analytical and numerical solutions are available for the hazard function even for the simplest dynamic system, i.e., deterministic linear elastic SDOF oscillator (Crandall, 1970). Extension of the functional form in Eq. (2) to the double-barrier problem is straightforward and can be formally expressed as

$$P_{f, |X|}(\zeta, t) = 1 - P[|X(t=0)| < \zeta] \cdot \exp\left\{-\int_0^t h_{|X|}(\zeta, \tau) d\tau\right\} \quad (3)$$

where $P_{f, |X|}(\zeta, t)$ and $h_{|X|}(\zeta, t)$ = time-variant probability of failure and hazard function, respectively, for process $|X(t)|$ and threshold level ζ . In this paper, both single- and double-barrier problems are considered. It is noticed here that, once the time-variant hazard function is known, the failure probability can be estimated by evaluating through numerical quadrature the time integrals in Eqs. (2) and (3).

The simplest approximation for the hazard function is the Poisson hazard function, $h_{X, P}(\zeta^+, t) = v_X(\zeta^+, t)$, obtained by assuming that the up-crossing events are statistically independent with their occurrence in time following a (memoryless) Poisson process. This assumption becomes increasingly accurate for increasing response threshold level and increasing bandwidth of the response process (e.g., as produced by increasing the damping level in a linear elastic system). For low threshold levels and/or narrow-band processes, the Poisson hazard function yields conservative values of the probability of failure. An improved estimate of the time-variant failure probability has been developed by Vanmarcke (1975), considering the envelope process as defined by Cramer and Leadbetter (1967). This improved estimate, referred to as classical Vanmarcke approximation, is based on the two-state Markov process assumption and takes into account (1) the fraction of time, termed fractional time, that the envelope process spends above the threshold level ζ , and (2) the fact that up-crossings of the envelope process are not always associated with one or more up-crossings of the process itself. The first consideration is important for low threshold levels, while the second consideration can be relevant for high threshold levels. The hazard function obtained for the non-stationary case is

$$h_{X,VM}(\zeta^+, t) = \nu_X(\zeta^+, t) \cdot \frac{1 - \exp\left[-\sqrt{2\pi} \cdot q(t) \cdot \frac{\zeta^+}{\sigma_X(t)}\right]}{1 - \exp\left[-\frac{1}{2} \left[\frac{\zeta^+}{\sigma_X(t)}\right]^2\right]} \quad (4)$$

where $q(t)$ = time-variant bandwidth parameter, and $\sigma_X(t)$ = time-variant standard deviation of process $X(t)$. Vanmarcke (1975) also suggested an empirical modification of Eq. (4), in which the bandwidth parameters $q(t)$ is substituted with $[q(t)]^{1.2}$, to account for super-clamping effects, leading to the modified Vanmarcke approximation

$$h_{X,mVM}(\zeta^+, t) = \nu_X(\zeta^+, t) \cdot \frac{1 - \exp\left[-\sqrt{2\pi} \cdot [q(t)]^{1.2} \cdot \frac{\zeta^+}{\sigma_X(t)}\right]}{1 - \exp\left[-\frac{1}{2} \left[\frac{\zeta^+}{\sigma_X(t)}\right]^2\right]} \quad (5)$$

The hazard functions for the double-barrier problem corresponding to those in Eqs. (4) and (5) were derived for Gaussian processes and are obtained by substituting in these equations ζ^+ with ζ , $\nu_X(\zeta^+, t)$ with $\nu_{|X|}(\zeta, t) = 2\nu_X(\zeta^+, t)$, and $\sqrt{2\pi}$ with $\sqrt{\pi/2}$. In the original formulation (Corotis et al. 1972, Vanmarcke 1975), the bandwidth parameter was computed from the convergent part of the integrals defining the geometric spectral moments of the process of interest. In this paper, the bandwidth parameter is correctly computed from the non-geometric spectral characteristics of the considered stochastic process (Michaelov et al. 1999a), and its exact closed form, derived in Barbato and Conte (2008), is given in the next section.

USE OF SPECTRAL CHARACTERISTICS IN STRUCTURAL RELIABILITY

The spectral characteristics of a process $X(t)$ are necessary in order to compute its mean up-crossing rates and hazard functions. The non-geometric spectral characteristics of two zero-mean random processes $X_1(t)$ and $X_2(t)$ considered jointly are defined as (Barbato and Conte 2008)

$$c_{ik,X_1X_2}(t) = \int_{-\infty}^{\infty} \Phi_{X_1^{(i)}X_2^{(k)}}(\omega, t) d\omega = \sigma_{X_1^{(i)}X_2^{(k)}}(t) \quad (6)$$

in which $\Phi_{X_1^{(i)}X_2^{(k)}}(\omega, t)$ = evolutionary cross-power spectral density (Priestley 1987) of processes $X_1^{(i)} = d^i X_1 / dt^i$ and $X_2^{(k)} = d^k X_2 / dt^k$, and $\sigma_{X_1^{(i)}X_2^{(k)}}(t)$ = time-variant cross-covariance of processes $X_1^{(i)}$ and $X_2^{(k)}$. The particular case $X_1(t) = X_2(t) = X(t)$ gives $c_{00,XX}(t) = \sigma_X^2(t)$, $c_{11,XX}(t) = \sigma_{\dot{X}}^2(t)$, and $c_{01,XX}(t) = \sigma_{X\dot{X}}(t) = \rho_{X\dot{X}}(t) \cdot \sigma_X(t) \cdot \sigma_{\dot{X}}(t)$, in which $\rho_{X\dot{X}}(t)$ = cross-correlation coefficient between process $X(t)$ and its first time-derivative $\dot{X}(t)$. A superposed dot denotes differentiation with respect to time. For the particular case $X_1(t) = X(t)$ and $X_2(t) = Y(t)$ = auxiliary process obtained as time modulation (by the same modulating function as the process $X(t)$) of the Hilbert transform of the stationary process embedded in $X(t)$ (Michaelov et al. 1999a), the first-order spectral characteristic $c_{01,XY}(t) = \sigma_{X\dot{Y}}(t)$ is obtained. The auxiliary process $Y(t)$ is commonly used to define the envelope and phase processes of a non-stationary process (Muscolino 1988). The time-variant bandwidth parameter $q(t)$ of process $X(t)$ is computed as

$$q(t) = \left[1 - \frac{\sigma_{X\dot{Y}}^2(t)}{\sigma_X^2(t) \cdot \sigma_{\dot{X}}^2(t)} \right]^{1/2} \quad (7)$$

Eq. (7) was derived in Barbato and Conte (2008) by extending the definition of the bandwidth parameter $q(t)$ for real-valued non-stationary processes (Michaelov et al. 1999a) to complex-valued non-stationary processes. It can be shown that the value of $q(t)$ defined in Eq. (7) is bounded between zero and one for real-valued processes, with values close to zero corresponding to narrow-band processes and values close to one corresponding to broad-band processes.

APPLICATION EXAMPLES

SDOF linear elastic oscillators

The first application example consists of a linear elastic SDOF oscillator subjected to a zero-mean Gaussian white noise base excitation time-modulated by a unit-step function, i.e., with at rest initial

conditions. For this problem, exact solutions for the time-variant spectral characteristics up to the second order are available in closed-form (Barbato and Conte 2008). Fig. 1 plots the normalized second-order stochastic moments of the displacement (relative to the base) $U(t)$ and its first time derivative $\dot{U}(t)$ of a linear elastic SDOF system with natural period $T_0 = 0.5\text{s}$ and damping ratio $\xi = 0.05$. These closed-form solutions are applied in this study to obtain exact time-variant mean up-crossing rates, as well as Poisson and Vanmarcke approximations to the time-variant failure probability for the double-barrier problem, as defined previously. The relative displacement response $U(t)$ of the system is a zero-mean Gaussian process, for which the exact time-variant mean up-crossing rate for a given deterministic threshold is available in closed-form. The effects on the failure probability of the system parameters (i.e., natural circular frequency, ω_0 , and damping ratio, ξ) and response threshold level (normalized with respect to the stationary value of the standard deviation of the response process as $\zeta/\sigma_{U\infty}$) are investigated using the closed-form solutions available. The effect of the intensity of the excitation can be obtained indirectly from the effect of the threshold level, since due to system linearity the response scales linearly with respect to the intensity or magnitude of the excitation as measured by the square root of the white noise power spectral density, $\sqrt{\Phi_0}$ [$\text{m/s}^{3/2}$].

Figs. 2 through 7 show some selected analysis results for the out-crossing of specified threshold levels (double-barrier problem) by the response of a linear elastic SDOF system with natural period $T_0 = 0.5\text{s}$ and damping ratio $\xi = 0.05$ subjected to a white noise base excitation of power spectral density $\Phi_0 = 1 \text{ m}^2/\text{s}^3$ from at rest initial conditions. Figs. 2, 4, and 6 plot the time-variant mean out-crossing rate, ν , the classical Vanmarcke hazard function, h_{VM} , and the modified Vanmarcke hazard function, h_{mVM} , for the relative displacement response process $U(t)$ of the linear elastic SDOF system defined above and response threshold levels $\zeta = 2\sigma_{U\infty}$, $3\sigma_{U\infty}$, and $4\sigma_{U\infty}$, respectively, in which $\sigma_{U\infty}$ = stationary standard deviation of response process $U(t)$. Figs. 3, 5, and 7 show for the same SDOF system the time-variant expected number of out-crossings, $E[N]$, and the time-variant failure probability estimates obtained from the Poisson approximation, $P_{f,p}$, the classical Vanmarcke approximation, $P_{f,VM}$, and the modified Vanmarcke

approximation, $P_{f, mVM}$, respectively. Figs. 3, 5, and 7 also provide the failure probability at different instants of time obtained by Importance Sampling using Elementary Events (ISEE) (Au and Beck 2001) with a coefficient of variation $c.o.v. = 0.01$, $P_{f, sim}$. The equations needed to compute the estimates of the failure probability, $P_{f, sim}$, and of its coefficient of variation, $c.o.v.(P_{f, sim})$, are taken from Au and Beck (2001). The value of $c.o.v.(P_{f, sim}) = 0.01$ was chosen in order to obtain accurate estimates of the time-variant failure probability. It is noteworthy that the computational time corresponding to each analytical approximate solution for the time history of the time-variant failure probability is several hundred times smaller than the computational time required to obtain the ISEE estimate of the time-variant failure probability at a single instant of time.

For the case corresponding to the threshold level $\zeta = 2\sigma_{U\infty}$, the hazard functions obtained using the classical and modified Vanmarcke approximations assume much lower values than the corresponding mean out-crossing rate, as shown in Fig. 2. For the very high values of the failure probability found in this case, the analytical upper bound provided by $E[N]$ is not useful, since the expected number of out-crossings is larger than one after about 3 seconds of white noise excitation, and the Poisson approximation largely overestimates the probability of failure (see Fig. 3). On the other hand, the two Vanmarcke approximations are both in good agreement with the simulation results, with better agreement reached by the classical Vanmarcke approximation for $t \leq 2.5s$ and by the modified Vanmarcke approximation for $t \geq 3.0s$. In this specific case, the failure probability at different instants of time was also computed using crude Monte Carlo Simulation (MCS), the use of which was possible due to the large values assumed by the time-variant probability of failure. The results obtained by crude MCS were found in very good agreement with those resulting from ISEE.

The mean out-crossing rate corresponding to the threshold $\zeta = 3\sigma_{U\infty}$ is larger than the classical and modified Vanmarcke hazard functions (see Fig. 4), but the relative differences are smaller than for lower response thresholds. It is also observed that as the response threshold increases, the time required for the mean out-crossing rate and the hazard functions to reach stationarity increases as well. From the

comparison of the analytical approximations of the time-variant failure probability with the accurate ISEE-based estimate thereof shown in Fig. 5, it is observed that: (1) the expected number of out-crossings (analytical upper bound of the failure probability) is almost double the failure probability obtained by ISEE and the Poisson approximation improves only slightly over the upper bound results; (2) the two Vanmarcke approximations provide good estimates of the failure probability, but in this case the classical Vanmarcke approximation is in better agreement overall with the ISEE results. Nevertheless, the ISEE results shift progressively away from the classical to the modified Vanmarcke approximation results as time elapses.

For the relative displacement response threshold $\zeta = 4\sigma_{U\infty}$, the relative differences between the Vanmarcke approximations and the mean out-crossing rate are smaller than for lower thresholds, as shown in Fig. 6. In this case, the expected number of out-crossings and the Poisson approximation practically coincide and their relative differences with the ISEE results are lower than in the previous two cases (see Fig. 7). The classical Vanmarcke approximation almost coincides with the ISEE results, while the modified Vanmarcke approximation underestimates the failure probability.

Fig. 8 compares the estimated relative displacement response hazard curves (i.e., failure probability versus normalized relative displacement threshold) with ISEE results for the considered linear elastic SDOF system subjected to 5.0s of white noise base excitation from at rest initial conditions. The failure probability estimates are computed based on the Poisson approximation as well as the classical and modified Vanmarcke approximations. The ISEE results have a coefficient of variation of 1% for the failure probability estimate and are therefore accurate. As expected from previous results available in the literature (Crandall 1970), it is observed that the two Vanmarcke approximations provide significantly improved estimates of the failure probability compared to the Poisson approximation, particularly in the threshold level range $2 \leq \zeta/\sigma_{U\infty} \leq 4$. For increasing threshold levels, all three approximations appear to converge asymptotically to the “exact” failure probability. Notice that the analytical relative displacement response hazard curves are computed for a constant threshold level increment of $0.1\sigma_{U\infty}$ and are obtained

at an extremely small fraction of the computational cost of the ISEE results. Table 1 reports the values of the time-variant failure probability estimated using the Poisson approximation, the classical and modified Vanmarcke approximations, and ISEE analysis for a linear elastic SDOF system with natural period $T_0 = 0.5s$, subjected to white noise base excitation from at rest initial conditions. Results are given for different normalized relative displacement response thresholds ($\zeta/\sigma_{U\infty} = 2, 3$, and 4 , i.e., the range in which the various approximations differ the most as shown in Fig. 8), several damping ratios ($\xi = 1\%, 5\%, 10\%$), and different exposure times (normalized with respect to the natural period, i.e., $5T_0$ and $10T_0$). From the results shown in Table 1, the following observations are made: (1) the two Vanmarcke approximations provide failure probability estimates in better agreement with the ISEE analysis results (i.e., more accurate) than the Poisson approximation; (2) the accuracy of the modified Vanmarcke approximation improves with increasing exposure time to the white noise excitation; (3) the relative accuracy of the two Vanmarcke approximations in estimating the failure probability depends on both the order of magnitude of the failure probability (for small failure probabilities, e.g., $P_f < 1e-4$, the classical Vanmarcke approximation is more accurate than the modified Vanmarcke approximation) and the damping ratio (for $\xi = 5\%$, the modified Vanmarcke approximation tends to be more accurate than the classical Vanmarcke approximation, for $\xi = 10\%$, the classical Vanmarcke approximation is more accurate than the modified Vanmarcke approximation, for $\xi = 1\%$ the more accurate of the two Vanmarcke approximations depends on the exposure time and the magnitude of the failure probability).

Three-dimensional asymmetric building (linear elastic MDOF system)

The idealized three-dimensional (3-D) asymmetric building shown in Fig. 9 is used in this study as benchmark problem of a linear elastic MDOF system. This building consists of three floor diaphragms, assumed infinitely rigid in their own plane, supported by wide flange steel columns of section $W14 \times 145$. Each floor diaphragm consists of an 18cm thick reinforced-concrete slab with a weight density of $36kN/m^3$. The axial deformations of the columns are neglected. The modulus of elasticity of steel is taken as 200GPa. The motion of each floor diaphragm is completely defined by three DOFs defined at its center

of mass, namely the relative displacements with respect to the ground in the x-direction, U_{xi} , and in the y-direction, U_{yi} , and the rotation about the vertical z-axis, Θ_{zi} , with $i = 1, 2, 3$. Both classically and non-classically damped structural models of this building are considered in this study. For the case of classical damping, each modal damping ratio is taken as 2%. To physically realize the non-classical damping case, diagonal viscous damping elements (e.g., fluid viscous braces) are added as shown in Fig. 9. The damping coefficient of each viscous damping element is taken as $0.1 \text{ kN}\cdot\text{s}/\text{mm}$. The undamped natural circular frequencies of this building are given in Table 2.

White noise base excitation

As first benchmark for linear elastic MDOF systems, the building considered here is subjected, from at rest initial conditions, to an earthquake ground motion (defined in terms of ground acceleration) acting at 45 degrees with respect to the x-axis and modeled as a white noise process with power spectral density $\Phi_0 = 0.0625 \text{ m}^2/\text{s}^3$. Figs. 10 through 20 show some selected results of the time-variant reliability analysis of the considered building structure with and without the viscous dampers. Three response quantities are considered: the horizontal displacement at the third floor in the x-direction, U_{x3} (Figs. 10 through 14), which is the weak direction of the building along which the dampers are active, the horizontal displacement at the third floor in the y-direction, U_{y3} (Figs. 15 through 17), which is the strong direction of the building, and the horizontal drift between the third and second floors in the x-direction, $\Delta_{x3} = U_{x3} - U_{x2}$ (Figs. 18 through 20). As in the first application example, the results presented here refer to the double-barrier first-passage problem for the considered response quantities.

Fig. 10 plots the time histories of the normalized variance and bandwidth parameter of U_{x3} for both the classically and non-classically damped 3-D asymmetric building. The displacement response variances are normalized with respect to the variance of U_{x3} at time $t = 5.0 \text{ s}$ for the classically damped system (i.e., building without viscous dampers). The addition of viscous dampers to the building produces two distinct effects on the variance of the response U_{x3} : (1) the variance is significantly reduced (at time $t = 5.0 \text{ s}$,

$\sigma_d^2/\sigma_u^2 = 0.39$), and (2) the response stationarity conditions are reached much faster. The effects of the viscous dampers on the time history of the bandwidth parameter are the reduction of the time needed to reach stationarity and the increase of the stationary value, which are consistent with the increase of damping in the system (see Barbato and Conte 2008).

Fig. 11 shows the time-variant mean out-crossing rate, ν , as well as the classical and modified Vanmarcke hazard functions (i.e., h_{VM} and h_{mVM} , respectively) for the DOF U_{X3} corresponding to the deterministic threshold $\zeta = 0.114m$ (i.e., roof drift ratio = 1%) and relative to the classically damped 3-D building. The two Vanmarcke hazard functions are significantly lower than the mean out-crossing rate function. Fig. 12 compares, for the same analysis case considered in Fig. 11, the various analytical approximations of the failure probability (i.e., expected number of out-crossings, $E[N]$, Poisson approximation, $P_{f,p}$, classical Vanmarcke approximation, $P_{f,VM}$, and modified Vanmarcke approximation, $P_{f,mVM}$) with the simulation results obtained using the ISEE method, $P_{f,sim}$. In this specific case, the simulation results are almost in perfect agreement with the modified Vanmarcke approximation. The failure probability after 5.0s of excitation is of the order of 1%. This failure probability (conditional on the given magnitude Φ_0 of the white noise ground motion excitation) is quite large and can be considered unsatisfactory for the given threshold, thus suggesting a retrofit of the building using the viscous damping system previously defined. Figs. 13 and 14 show the same information as in Figs. 11 and 12, respectively, but for the case of the non-classically damped building (i.e., building with viscous dampers). The mean out-crossing rate and hazard functions are four orders of magnitude lower and the failure probability estimates seven orders of magnitude lower than for the classically damped building (i.e., building without viscous dampers). Here, the classical Vanmarcke approximation is in better agreement with the ISEE results (i.e., more accurate) than the modified Vanmarcke approximation; it slightly underestimates the time-variant failure probability. In this case, the effectiveness of viscous dampers in reducing the probability of DOF U_{X3} out-crossing the level considered is noteworthy.

Fig. 15 plots the time histories of the normalized variance and bandwidth parameter of U_{Y3} for both the

classically and non-classically damped 3-D asymmetric building. The displacement response variances are normalized with respect to the variance of U_{Y3} at time $t = 5.0s$ for the classically damped system. The effects of the viscous dampers on the statistics of U_{Y3} are very small and consist of a small reduction in the variance of U_{Y3} , while the changes in the time history of the bandwidth parameter are not visible at the scale used in Fig. 15. This result was expected, since the action of the viscous dampers is directed along the x-direction of the building and affects the y-direction only indirectly, through the coupling with the torsional modes of vibration. Figs. 16 and 17 provide a comparison of the various analytical approximations with the ISEE-based estimate of the failure probability related to U_{Y3} and threshold $\zeta = 0.114m$ for the classically and non-classically damped 3-D asymmetric building, respectively. In this case, the failure probability is already very small for the classically damped building and reduces further by a factor of two for the non-classically damped building. The simulation results lie between the estimates from the classical and modified Vanmarcke approximations.

Fig. 18 shows the time histories of the normalized variance and bandwidth parameter of the interstory drift Δ_{X3} for both the classically and non-classically damped 3-D asymmetric building. The drift response variances are normalized with respect to the variance of Δ_{X3} at time $t = 5.0s$ for the classically damped system. Variances and bandwidth parameters for drifts and any other response quantities linearly related to displacement responses can be computed directly from the variances and bandwidth parameters of the latter quantities (Barbato and Conte 2008). Regarding the normalized variance and bandwidth parameter of Δ_{X3} , it is observed that: (1) the variance of the drift response is much lower for the non-classically damped than for the classically damped building, (2) stationarity is reached faster for the non-classically damped building, and (3) the stationary value of the bandwidth parameter is lower for the non-classically damped than for the classically damped building. This last observation (which could appear counter-intuitive) is due to the fact that although the non-classically damped building has higher modal damping ratios (and therefore modal responses with broader bandwidth), its first mode is more predominant than in the case of the classically damped building. In other words, the stationary value of the central frequency

of each floor relative displacement response process is closer to the natural frequency of the predominant mode of vibration in the non-classically damped than in the classically damped building (see Barbato and Conte 2008). Figs. 19 and 20 compare the various analytical approximations with the ISEE-based estimate of the failure probability for Δ_{x3} and threshold $\zeta = 0.0285\text{m}$ (corresponding to an interstory drift ratio of 0.75%) for the classically and non-classically damped 3-D building, respectively. For the classically damped building, all the analytical approximations overestimate the failure probability obtained via the ISEE method, while for the non-classically damped building, the ISEE-based results lie between the classical and modified Vanmarcke approximations. Also for the response quantity Δ_{x3} , the use of viscous dampers produces a considerable reduction in the time-variant failure probability (five orders of magnitude). Also in this second application example, it is observed that the two Vanmarcke approximations of the time-variant failure probability are significantly more accurate than the Poisson approximation.

Time-modulated colored noise base excitation

In order to study the relative accuracy of different analytical approximations of the time-variant failure probability in the case of strongly non-stationary input excitations, the benchmark building model is subjected to a stochastic earthquake base excitation modeled as a time-modulated colored noise process. In this work, the Kanai-Tajimi spectrum (Clough and Penzien 1993) is used to model the basic stationary colored noise process. The Kanai-Tajimi spectrum represents the stochastic process obtained by filtering a white noise process through a linear filter representing the effects of a soil layer between the bedrock and the ground surface. It is expressed as

$$\Phi_{A_g A_g}(\omega) = \Phi_0 \cdot \left[\frac{\omega_g^4 + 4 \cdot \xi_g^2 \cdot \omega_g^2 \cdot \omega^2}{(\omega_g^2 - \omega^2)^2 + 4 \cdot \xi_g^2 \cdot \omega_g^2 \cdot \omega^2} \right] \quad (8)$$

where $\Phi_{A_g A_g}(\omega)$ denotes the PSD function of the ground surface acceleration process, $\Phi_0 = 0.0625\text{m}^2/\text{s}^3$ is

the intensity of the ideal white noise acceleration at the base of the soil layer, and $\omega_g = 12.5\text{rad/s}$ and ξ_g

$= 0.6$ represent the natural frequency and damping ratio, respectively, of the soil layer. Thus, ω_g and ξ_g are measures of the predominant frequency and bandwidth, respectively, of the ground surface acceleration.

The ground motion input to the structure is made non-stationary in amplitude by using the well known time-modulating function of Shinozuka and Sato (Shinozuka and Sato 1967) defined as

$$A_{a_g}(t) = C \cdot [\exp(-B_1 \cdot t) - \exp(-B_2 \cdot t)] \quad (9)$$

where $A_{a_g}(t)$ is the time-modulating function, and $C = 25.81$, $B_1 = 0.045\pi$, and $B_2 = 0.05\pi$ are constants defining the shape of the time-modulating function.

Fig. 21 plots the first 30s of the time histories of the normalized variance and bandwidth parameter of U_{X3} for both the classically and non-classically damped 3-D asymmetric building. The displacement response variances are normalized with respect to the maximum value assumed by the variance of U_{X3} for the classically damped system (i.e., $\sigma_{u,max}^2$). The addition of viscous dampers to the building produces two distinct effects on the variance of the response U_{X3} : (1) the variance is strongly reduced ($\sigma_{d,max}/\sigma_{u,max} = 0.63$, $\sigma_{u,max}/H = 0.31\%$, $\sigma_{d,max}/H = 0.20\%$, where the height of the building $H = 11.4m$), and (2) its peak value is reached earlier. The effects of the viscous dampers on the time history of the bandwidth parameter are the reduction of the time needed to reach the asymptotic value and the increase of the asymptotic value. This last effect is the same as the one observed in the case of white noise excitation for the stationary value of the bandwidth parameter of the response process U_{X3} (see Fig. 10).

Fig. 22 shows the time-variant mean out-crossing rate, v , as well as the classical and modified Vanmarcke hazard functions (i.e., h_{VM} and h_{mVM} , respectively) for the DOF U_{X3} corresponding to the deterministic threshold $\zeta = 0.114m$ and relative to the classically damped 3-D building. The two Vanmarcke hazard functions assume values significantly lower than the mean out-crossing rate function. For the same analysis case, Fig. 23 compares expected number of out-crossings, $E[N]$, Poisson approximation, $P_{f,p}$,

classical Vanmarcke approximation, $P_{f, VM}$, modified Vanmarcke approximation, $P_{f, mVM}$, and simulation results obtained using the ISEE method, $P_{f, sim}$. The ISEE simulation results are in good agreement with the modified Vanmarcke approximation. The failure probability after 30.0s of excitation is about 5%, thus justifying also in this case the need to retrofit the building using the viscous damping system previously defined. Figs. 24 and 25 show the same information as Figs. 22 and 23, respectively, but for the case of the building retrofitted with viscous dampers. The mean out-crossing rate function, hazard functions, and time-variant failure probability estimates are more than three orders of magnitude lower than for the building without viscous dampers. It is observed that the ISEE results lie between the Poisson and the classical Vanmarcke approximations. Also in this case, the effectiveness of the viscous dampers in reducing the probability of DOF U_{X3} out-crossing the level considered is noteworthy.

CONCLUSIONS

This paper presents the application of spectral characteristics of non-stationary random processes to the time-variant first-passage problem in structural reliability. The first-passage problem is applied to linear elastic models of structural systems and consists of computing the probability of exceeding a given deterministic time-invariant threshold by a response quantity (linearly) related to the displacement and velocity responses (e.g., absolute displacement, relative displacement, elastic force) of the system. This quantity is generally known as time-variant failure probability. Both the classical and modified Vanmarcke approximations are computed, through integration (using numerical quadrature) of the closed-form solutions for the corresponding approximate hazard functions, for linear elastic single-degree-of-freedom (SDOF) and multi-degree-of-freedom (MDOF) systems subjected to stationary and non-stationary base excitation from at rest initial conditions. The closed-forms of the two Vanmarcke hazard functions are obtained using the closed-form solutions for the time-variant bandwidth parameter characterizing the non-stationary stochastic process representing the displacement response considered. These approximate solutions for the time-variant failure probability are compared with the well known Poisson approximation and accurate simulation results obtained via the Importance Sampling using

Elementary Events (ISEE) method for two application examples: (1) a set of linear elastic SDOF systems, with different natural periods, damping ratios and response threshold levels, and (2) an idealized yet realistic three-dimensional asymmetric steel building model, both subjected to white noise base excitation from at rest initial conditions. For the second application example, retrofit of the given building with viscous dampers is also considered, serving a two-fold purpose: (1) to illustrate the use of the newly available closed-form approximations of the failure probability for non-classically damped linear elastic systems, and (2) to show an example of practical use in structural engineering of the presented analytical derivations.

The originality of the work presented here stems from the use, in the classical and modified Vanmarcke approximations to the first-passage reliability problem, of recently obtained exact closed-form solutions for the time-variant bandwidth parameter of the response of classically and non-classically damped linear elastic systems. To the authors' knowledge, this is the first time that the exact closed-form solutions for the Vanmarcke approximations are presented for non-stationary random vibration problems. Based on benchmark examples, these analytical approximate solutions are then compared with accurate simulation results obtained from the relatively recent Importance Sampling using Elementary Events (ISEE) method, allowing a confident appraisal of their absolute and relative accuracy under different conditions and especially in non-stationary random vibration. It is noteworthy that the computational cost of the presented closed-form analytical approximations of the time-variant failure probability is several orders of magnitude smaller than the one associated with the ISEE simulation method. From the results presented in this study, it is observed that the two Vanmarcke approximations provide estimates of the time-variant failure probability for the first-passage problem that are significantly more accurate than the simpler Poisson approximation and the analytical upper bound. On the other hand, the relative accuracy of the classical and modified Vanmarcke approximations can be evaluated only on a case by case basis and deserves further studies to be better understood. The accuracy of the two analytical Vanmarcke approximations of the time-variant failure probability is sufficient for common engineering applications. These closed-form approximations of the time-variant failure probability provide benchmark solutions

particularly useful to validate, in the elastic range, numerical solutions required for the first-passage problem associated with the non-stationary response of nonlinear hysteretic structural systems subjected to stochastic loading. In addition, the small computational cost of these closed-form analytical approximations renders them very valuable for practical purposes, e.g., for design-oriented parametric studies.

ACKNOWLEDGEMENTS

The authors gratefully acknowledge support of this research by (1) the National Science Foundation under Grant No. CMS-0010112, (2) the Pacific Earthquake Engineering Research (PEER) Center through the Earthquake Engineering Research Centers Program of the National Science Foundation under Award No. EEC-9701568, and (3) the Louisiana Board of Regents through the Pilot Funding for New Research Program of the National Science Foundation Experimental Program to Stimulate Competitive Research under Award No. NSF(2008)-PFUND-86. Any opinions, findings, conclusions or recommendations expressed in this publication are those of the authors and do not necessarily reflect the views of the sponsors.

REFERENCES

- AASHTO (1998). "AASHTO LRFD bridge design specification." American Association of State Highway and Transportation Officials, 2nd ed.
- ATC-58 (2005). "Development of next-generation performance-based seismic design procedures for new and existing buildings." Advanced Technology Council, Redwood City, CA.
- Au, S.K., and Beck, J.L. (2001a). "First excursion probabilities for linear systems by very efficient importance sampling." *Probabilistic Engineering Mechanics*, 16(3):193-207.
- Au, S.K., and J. L. Beck, J.L. (2001b). "Estimation of small failure probabilities in high dimensions by subset simulation." *Probabilistic Engineering Mechanics*, 16(4):263-277.
- Barbato, M., and Conte J.P. (2008). "Spectral Characteristics of Non-Stationary Random Processes: Theory and Applications to Linear Structural Models." *Probabilistic Engineering Mechanics*, 23(4):416-426.
- Barbato, M., Gu, Q., and Conte, J.P. (2008). "Extension of the DP-RS-Sim hybrid method to time-variant structural reliability analysis." *American Institute of Physics Proceedings*, 2008 Seismic Engineering International Conference (MERCEA'08), July 8-11, 2008, Messina (Italy).
- Barbato, M., and Vasta, M. (2010). "Closed-form solutions for the time-variant spectral characteristics of non-stationary random processes." *Probabilistic Engineering Mechanics*, 25(1):9-17.
- BSSC (2004). "The 2003 NEHRP recommended provisions for new buildings and other structures. Part 1: provisions (FEMA 450)." Building Seismic Science Council, <http://www.bssconline.org/>
- Ching, J., Au, S.K., and Beck, J.L. (2005). "Reliability estimation for dynamical systems subject to stochastic excitation using Subset Simulation with splitting." *Computer Methods in Applied Mechanics and Engineering*, 194(12-16):1557-1579.
- Clough, R.W., and Penzien, J. (1993). *Dynamics of Structures*. New York, USA: McGraw-Hill, 2nd Ed.

- Conte, J.P. (1992). "Effects of Earthquake Frequency Nonstationarity on Inelastic Structural Response." *Proceedings, 10th World Conference on Earthquake Engineering*, Madrid, Spain. Rotterdam: AA Balkema, 1992:3645-3651.
- Cornell, C.A., and Krawinkler, H. (2000). "Progress and challenges in seismic performance assessment." *PEER Center News*, Spring 2000.
- Corotis, R.B., Vanmarcke, E.H., and Cornell, C.A. (1972). "First passage of nonstationary random processes." *Journal of the Engineering Mechanics Division*, ASCE, 98(EM2):401-414.
- Cramer H., Leadbetter, M.R. (1967). *Stationary and related stochastic process*. New York, NY: Wiley.
- Crandall, S.H. (1970). "First-crossing probabilities of the linear oscillator." *Journal of Sounds and Vibrations*, 12(3):285-299.
- Di Paola, M. (1985). "Transient spectral moments of linear systems." *SM Archives*, 10:225-243.
- Fujimura, K., and Der Kiureghian, A. (2007). "Tail-equivalent linearization method for nonlinear random vibration." *Probabilistic Engineering Mechanics*, 22(1):63-76.
- Hagen, O., and Tvedt, L. (1991) "Vector process out-crossing as parallel system sensitivity measure." *Journal of Engineering Mechanics*, ASCE, 117(10):2201-2220.
- ICC (2003). "International Building Code 2003." International Code Council, CD-Rom.
- Katafygiotis, L.S., and Cheung, S.H. (2005). "A two-stage subset-simulation-based approach for calculating the reliability of inelastic structural systems subjected to Gaussian random excitations." *Computer Methods in Applied Mechanics and Engineering*, 194(12-16):1581-1595.
- Lin, Y.K. (1976). *Probabilistic Theory of Structural Dynamics*. New York, NY: McGraw-Hill, 1967, Huntington: Krieger Pub., 1976.
- Lutes, L.D., Sarkani S. (1997). *Stochastic analysis of structural and mechanical vibration*. Upper Saddle River, NJ: Prentice Hall.

- Michaelov, G., Sarkani, S., Lutes, L.D. (1999a). "Spectral characteristics of nonstationary random processes - a critical review." *Structural Safety*, 21(3):223-244.
- Michaelov, G., Sarkani, S., Lutes, L.D. (1999b). "Spectral characteristics of nonstationary random processes - response of a simple oscillator." *Structural Safety*, 21(3):245-267.
- Moehle, J., and Deierlein, G.G. (2004). "A framework methodology for Performance-Based Earthquake Engineering." *Proceedings, 13th World Conference on Earthquake Engineering*, Vancouver, Canada, August 1-6, 2004.
- Muscolino, G. (1988). "Nonstationary envelope in random vibration theory." *Journal of Engineering Mechanics*, ASCE, 114(8): 1396-1413.
- Naess, A., and Moe, V. (2000). "Efficient path integration methods for nonlinear dynamic systems." *Probabilistic Engineering Mechanics*, 15(2):221-231.
- Naess, A., Leira, B.J., and Batsevych, O. (2009). "System reliability analysis by enhanced Monte Carlo simulation." *Structural Safety*, 31(5):349-355.
- Papadimitriou, C. (1990). "Stochastic characterization of strong ground motion and applications to structural response." *Report No. EERL 90-03*, California Institute of Technology, Pasadena, CA.
- Pradlwarter, H.J., and Schueller, G.I. (2004). "Excursion probability of non-linear systems." *International Journal of Non-Linear Mechanics*, 39(9):1447-1452.
- Pradlwarter, H.J., Schueller, G.I., Koutsourelakis, P.S., and Charnpis, D.C. (2007). "Application of line sampling simulation method to reliability benchmark problems." *Structural Safety*, 29(3):208-221.
- Priestley, M.B. (1987). *Spectral Analysis and Time Series, Volume 1: Univariate Series, Volume 2: Multivariate Series, Prediction and Control*. London: Academic Press, Fifth Printing.
- Shinozuka, M., and Sato, Y. (1967). "Simulation of nonstationary random processes." *Journal of the Engineering Mechanics Division*, ASCE, 93(EM1):11-40.

- Rice, S.O. (1944). "Mathematical analysis of random noise." *Bell System Technical Journal*, 23:282-332.
- Rice, S.O. (1945). "Mathematical analysis of random noise - Conclusions." *Bell System Technical Journal*, 24:46-156.
- Vanmarcke, E.H. (1975). "On the distribution of the first-passage time for normal stationary random processes." *Journal of Applied Mechanics*, ASME, 42(2):215-220.
- Wen, Y.K. (1987). "Approximate methods for nonlinear time-variant reliability analysis." *Journal of Engineering Mechanics*, ASCE, 113(12):1826-1839.
- Yeh, C.-H. and Wen, Y.K. (1990). "Modeling of nonstationary ground motion and analysis of inelastic structural response." *Structural Safety*, 8:281-298.

TABLE CAPTIONS

- Table 1. Time-variant failure probability for linear elastic SDOF system with natural period $T_0 = 0.5s$ subjected to white noise base excitation from at rest initial conditions
- Table 2. Undamped natural frequencies and description of vibration mode shapes of the three-dimensional asymmetric building example

FIGURE CAPTIONS

- Figure 1. Second-order stochastic moments of the response of linear elastic SDOF system with natural period $T_0 = 0.5s$ and damping ratio $\xi = 0.05$ (Y denotes the auxiliary process of process U).
- Figure 2. Mean up-crossing rate, classical and modified Vanmarcke hazard functions of the relative displacement response of linear elastic SDOF system with natural period $T_0 = 0.5s$ and damping ratio $\xi = 0.05$ relative to threshold level $\zeta = 2.0\sigma_{U\infty}$.
- Figure 3. Approximations of time-variant failure probability of linear elastic SDOF system with natural period $T_0 = 0.5s$ and damping ratio $\xi = 0.05$ for relative displacement threshold level $\zeta = 2.0\sigma_{U\infty}$.
- Figure 4. Mean up-crossing rate, classical and modified Vanmarcke hazard functions of the relative displacement response of linear elastic SDOF system with natural period $T_0 = 0.5s$ and damping ratio $\xi = 0.05$ relative to threshold level $\zeta = 3.0\sigma_{U\infty}$.
- Figure 5. Approximations of time-variant failure probability of linear elastic SDOF system with natural period $T_0 = 0.5s$ and damping ratio $\xi = 0.05$ for relative displacement threshold level $\zeta = 3.0\sigma_{U\infty}$.
- Figure 6. Mean up-crossing rate, classical and modified Vanmarcke hazard functions of the relative displacement response of linear elastic SDOF system with natural period $T_0 = 0.5s$ and

damping ratio $\xi = 0.05$ relative to threshold level $\zeta = 4.0\sigma_{U_{\infty}}$.

Figure 7. Approximations of time-variant failure probability of linear elastic SDOF system with natural period $T_0 = 0.5s$ and damping ratio $\xi = 0.05$ for relative displacement threshold level $\zeta = 4.0\sigma_{U_{\infty}}$.

Figure 8. Comparison between relative displacement response hazard curves obtained via Poisson approximation, classical and modified Vanmarcke approximations, and ISEE results for linear elastic SDOF system with natural period $T_0 = 0.5s$ and damping ratio $\xi = 0.05$.

Figure 9. Three-dimensional asymmetric building: (a) geometry, (b) floor view.

Figure 10. Normalized variance and bandwidth parameter of horizontal displacement response in x-direction at third floor (DOF U_{x3}) for classically (subscript 'u') and non-classically (subscript 'd') damped three-dimensional asymmetric building subjected to white noise base excitation.

Figure 11. Mean out-crossing rate, classical and modified Vanmarcke hazard functions for the DOF U_{x3} and deterministic threshold $\zeta = 0.114m$ (classically damped 3-D building subjected to white noise base excitation).

Figure 12. Comparison of analytical approximations with ISEE estimate of the time-variant failure probability for DOF U_{x3} and deterministic threshold $\zeta = 0.114m$ (classically damped 3-D building subjected to white noise base excitation).

Figure 13. Mean out-crossing rate, classical and modified Vanmarcke hazard functions for the DOF U_{x3} and deterministic threshold $\zeta = 0.114m$ (non-classically damped 3-D building subjected to white noise base excitation).

Figure 14. Comparison of analytical approximations with ISEE estimate of the time-variant failure

probability for DOF U_{X3} and deterministic threshold $\zeta = 0.114\text{m}$ (non-classically damped 3-D building subjected to white noise base excitation).

Figure 15. Normalized variance and bandwidth parameter of horizontal displacement response in y-direction at third floor (DOF U_{Y3}) for classically (subscript 'u') and non-classically (subscript 'd') damped three-dimensional asymmetric building subjected to white noise base excitation.

Figure 16. Comparison of analytical approximations with ISEE estimate of the time-variant failure probability for DOF U_{Y3} and deterministic threshold $\zeta = 0.114\text{m}$ (classically damped 3-D building subjected to white noise base excitation).

Figure 17. Comparison of analytical approximations with ISEE estimate of the time-variant failure probability for DOF U_{Y3} and deterministic threshold $\zeta = 0.114\text{m}$ (non-classically damped 3-D building subjected to white noise base excitation).

Figure 18. Normalized variance and bandwidth parameter of horizontal drift in the x-direction between third and second floors ($\Delta_{X3} = U_{X3} - U_{X2}$) for classically (subscript 'u') and non-classically (subscript 'd') damped 3-D building subjected to white noise base excitation.

Figure 19. Comparison of analytical approximations with ISEE estimate of the time-variant failure probability for Δ_{X3} and deterministic threshold $\zeta = 0.114\text{m}$ (classically damped 3-D building subjected to white noise base excitation).

Figure 20. Comparison of analytical approximations with ISEE estimate of the time-variant failure probability for Δ_{X3} and deterministic threshold $\zeta = 0.114\text{m}$ (non-classically damped 3-D building subjected to white noise base excitation).

Figure 21. Normalized variance and bandwidth parameter of horizontal displacement response in x-direction at third floor (DOF U_{X3}) for classically (subscript 'u') and non-classically (subscript

‘d’) damped three-dimensional asymmetric building subjected to time-modulated colored noise base excitation.

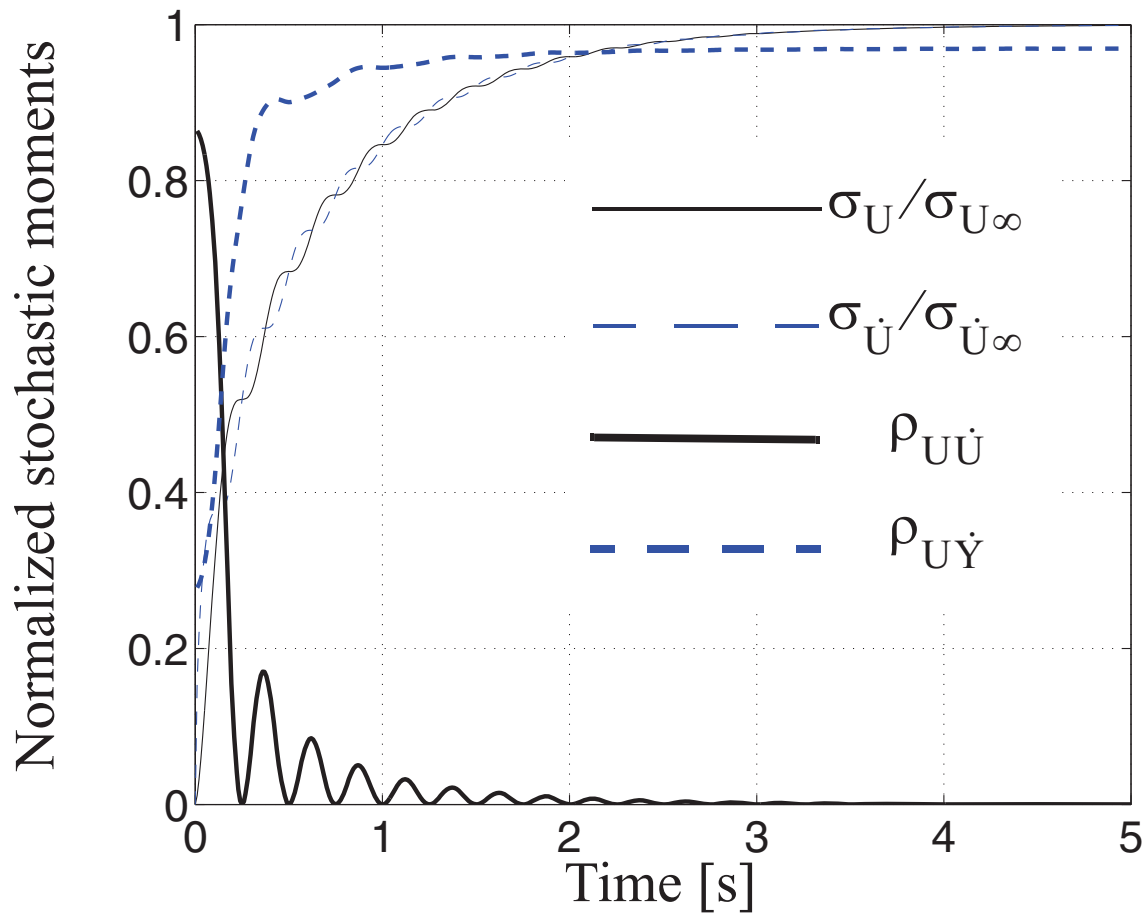
Figure 22. Mean out-crossing rate, classical and modified Vanmarcke hazard functions for the DOF U_{X3} and deterministic threshold $\zeta = 0.114\text{m}$ (classically damped 3-D building subjected to time-modulated colored noise base excitation).

Figure 23. Comparison of analytical approximations with ISEE estimate of the time-variant failure probability for DOF U_{X3} and deterministic threshold $\zeta = 0.114\text{m}$ (classically damped 3-D building subjected to time-modulated colored noise base excitation).

Figure 24. Mean out-crossing rate, classical and modified Vanmarcke hazard functions for the DOF U_{X3} and deterministic threshold $\zeta = 0.114\text{m}$ (non-classically damped 3-D building subjected to time-modulated colored noise base excitation).

Figure 25. Comparison of analytical approximations with ISEE estimate of the time-variant failure probability for DOF U_{X3} and deterministic threshold $\zeta = 0.114\text{m}$ (non-classically damped 3-D building subjected to time-modulated colored noise base excitation).

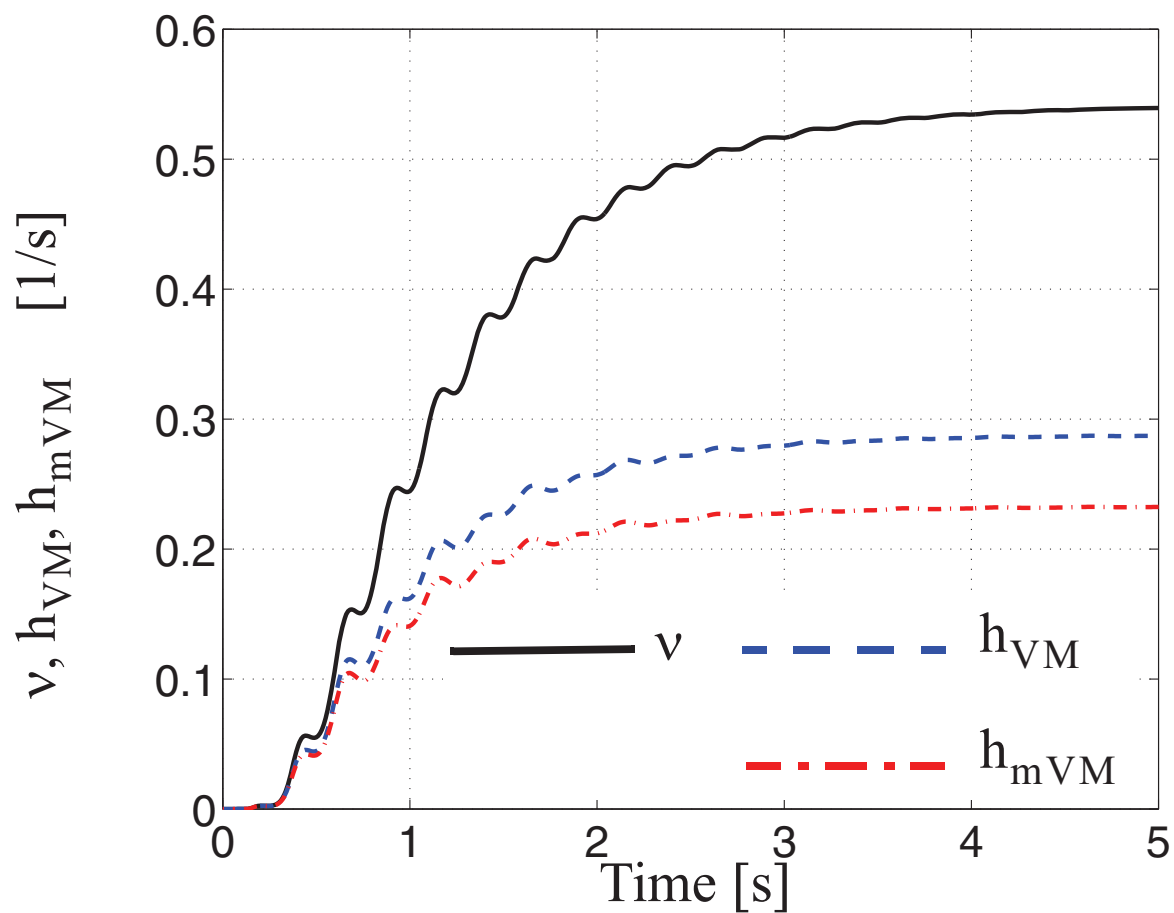
Figure 1



Accepted Manuscript
Not Copyedited

Figure 2

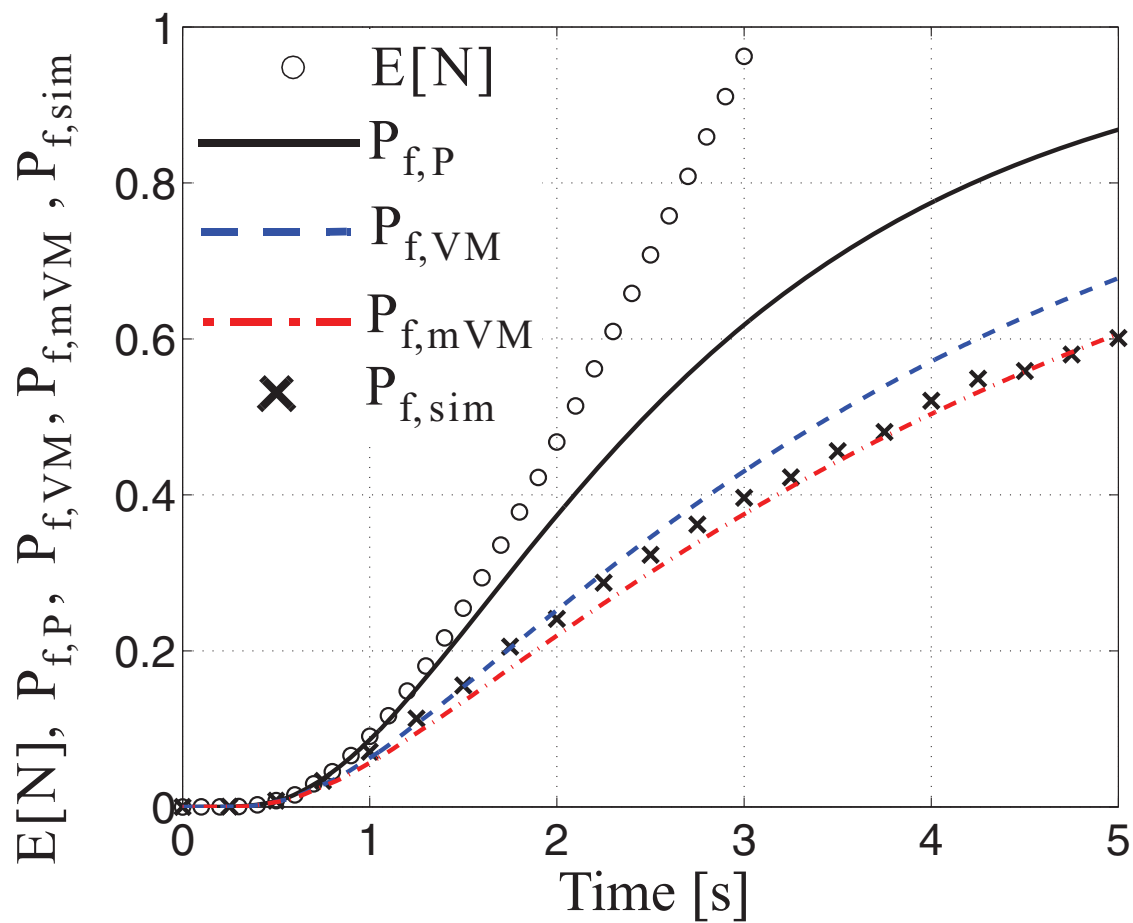
Journal of Engineering Mechanics. Submitted August 22, 2009; accepted November 16, 2010;
posted ahead of print November 18, 2010. doi:10.1061/(ASCE)EM.1943-7889.0000238



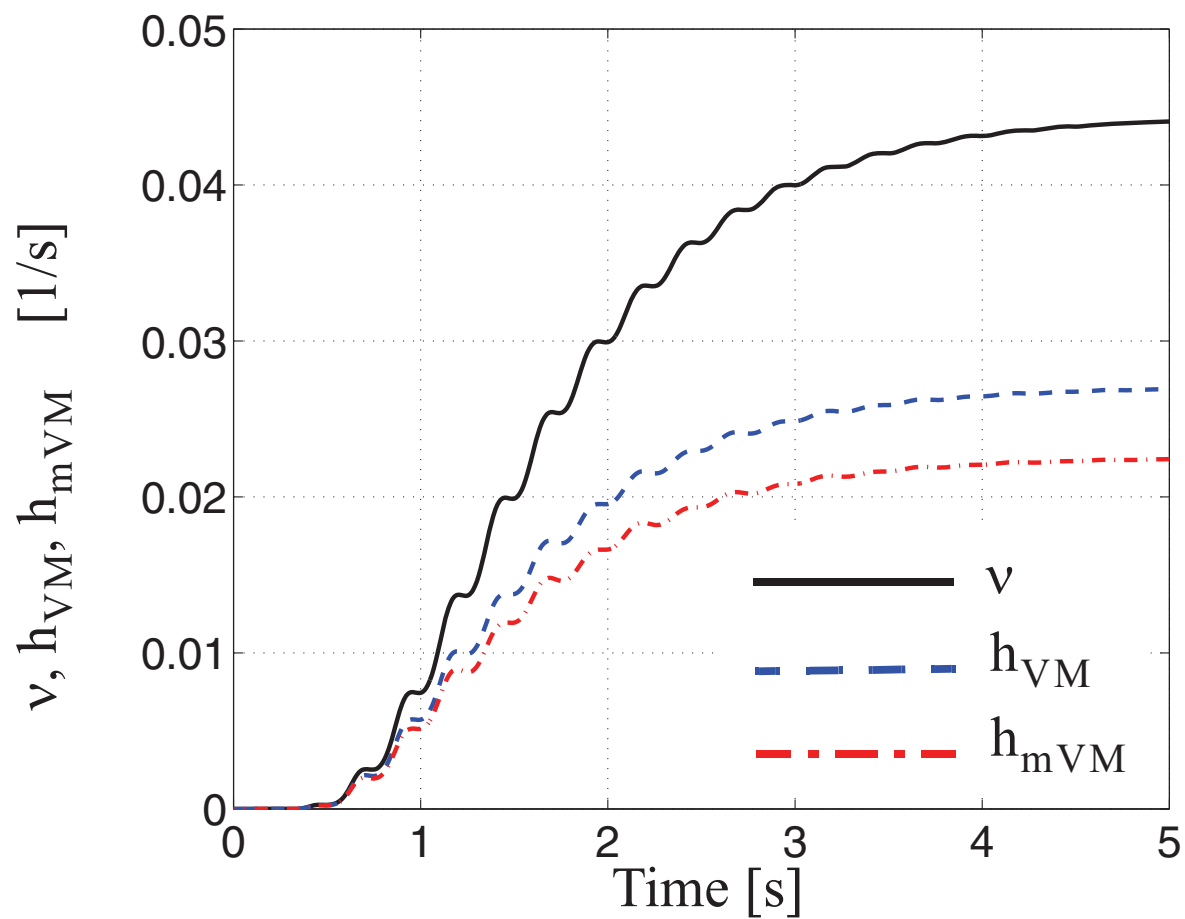
Accepted Manuscript
Not Copyedited

Figure 3

Journal of Engineering Mechanics. Submitted August 22, 2009; accepted November 16, 2010;
posted ahead of print November 18, 2010. doi:10.1061/(ASCE)EM.1943-7889.0000238

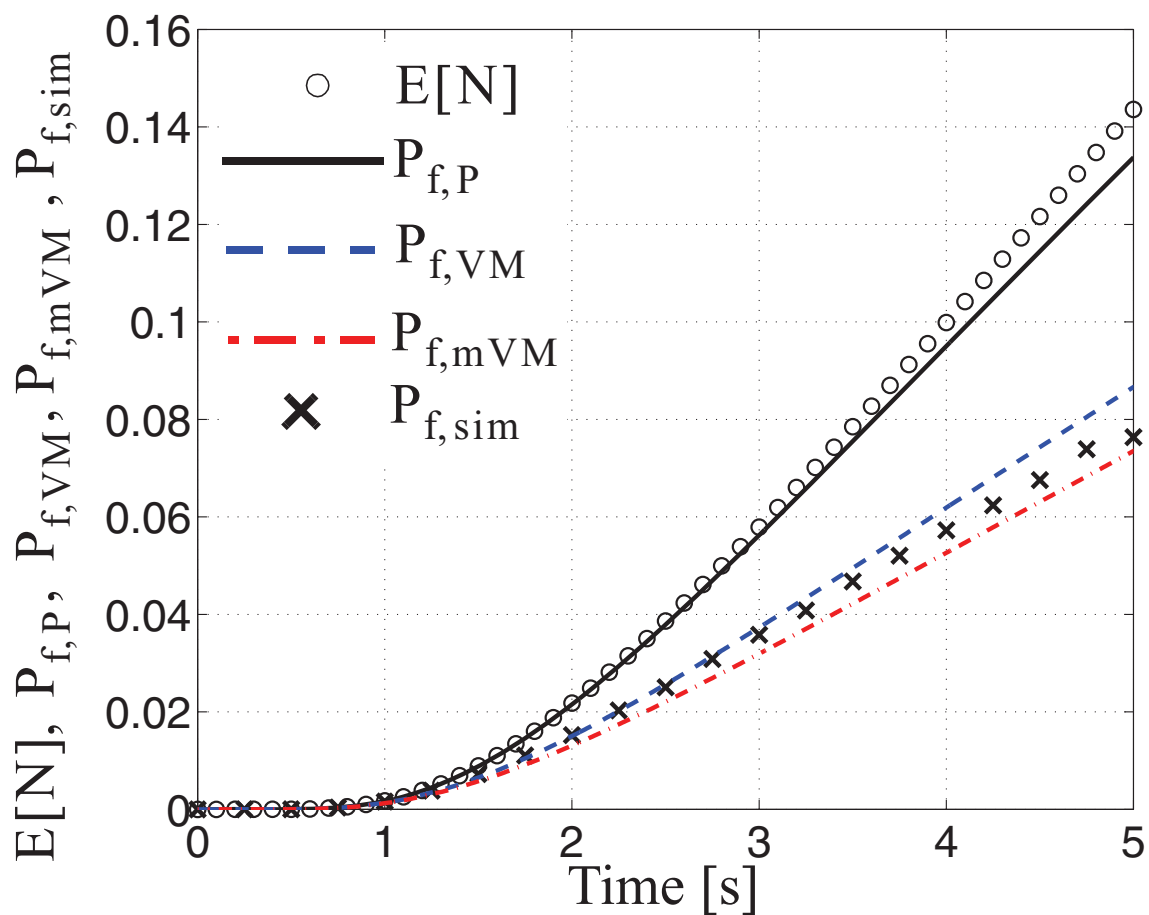


Accepted Manuscript
Not Copyedited



Accepted Manuscript
Not Copyedited

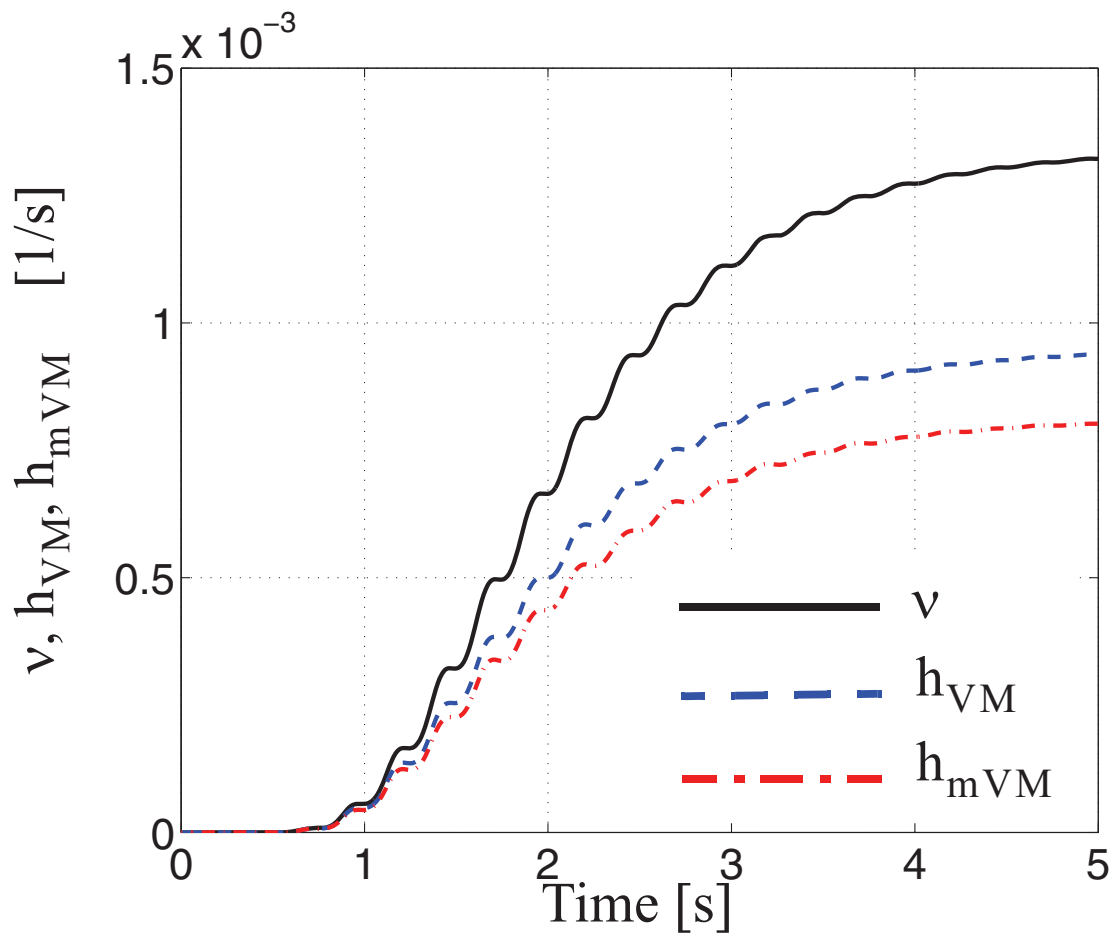
Figure 5



Accepted Manuscript
Not Copyedited

Figure 6

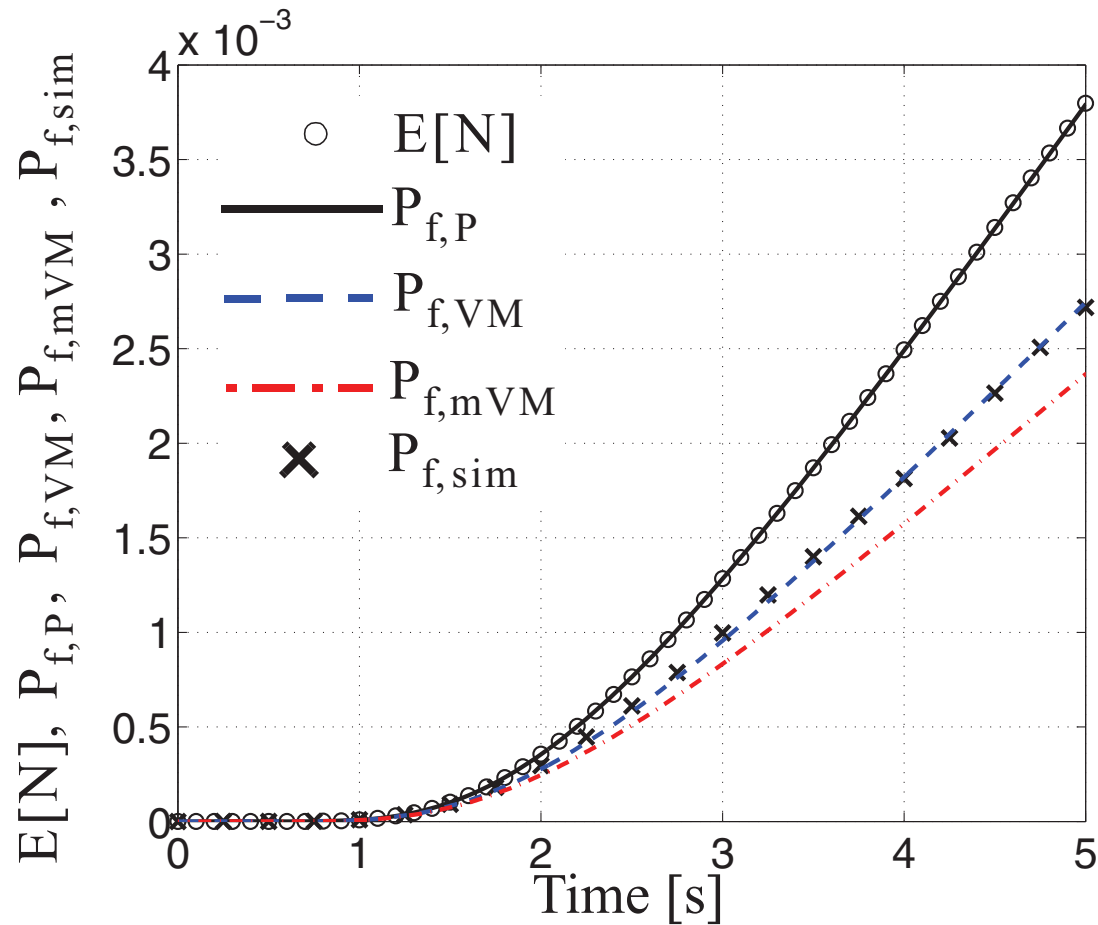
Journal of Engineering Mechanics. Submitted August 22, 2009; accepted November 16, 2010;
posted ahead of print November 18, 2010. doi:10.1061/(ASCE)EM.1943-7889.0000238



Accepted Manuscript
Not Copyedited

Figure 7

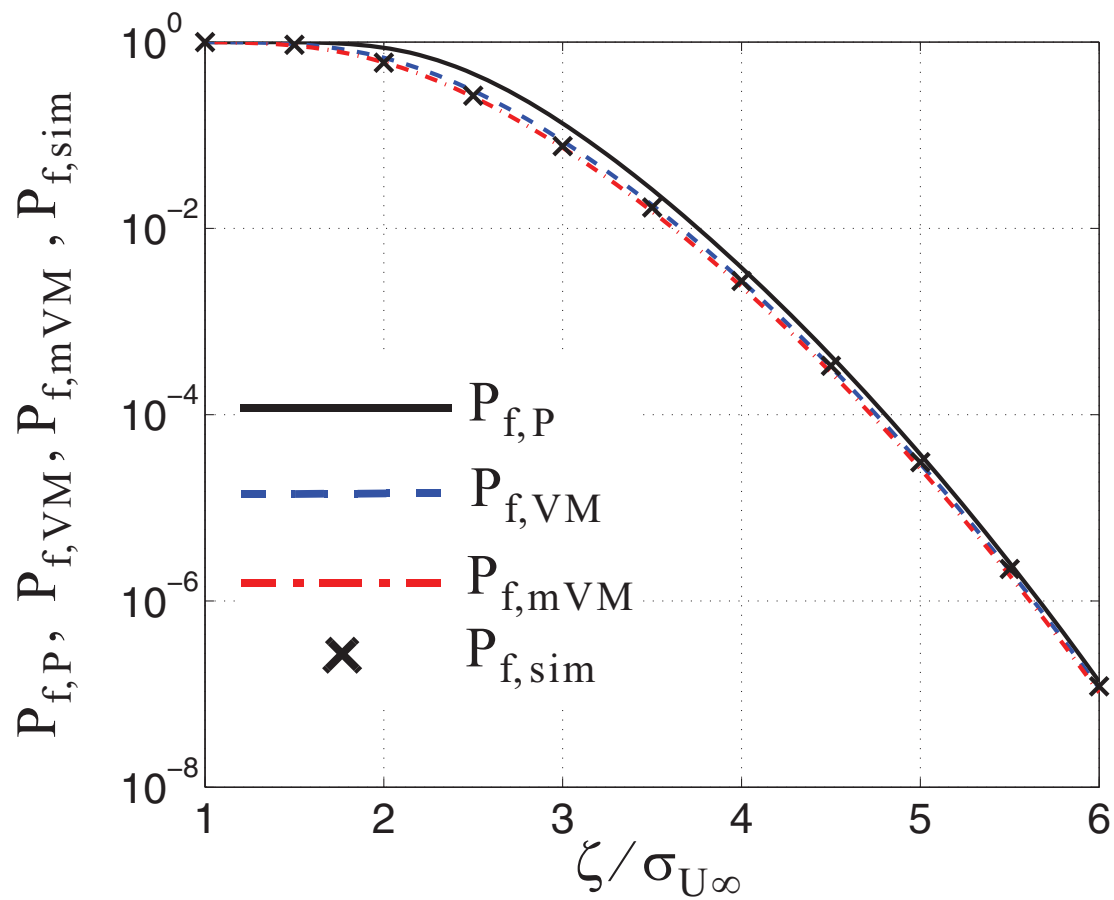
Journal of Engineering Mechanics. Submitted August 22, 2009; accepted November 16, 2010;
posted ahead of print November 18, 2010. doi:10.1061/(ASCE)EM.1943-7889.0000238



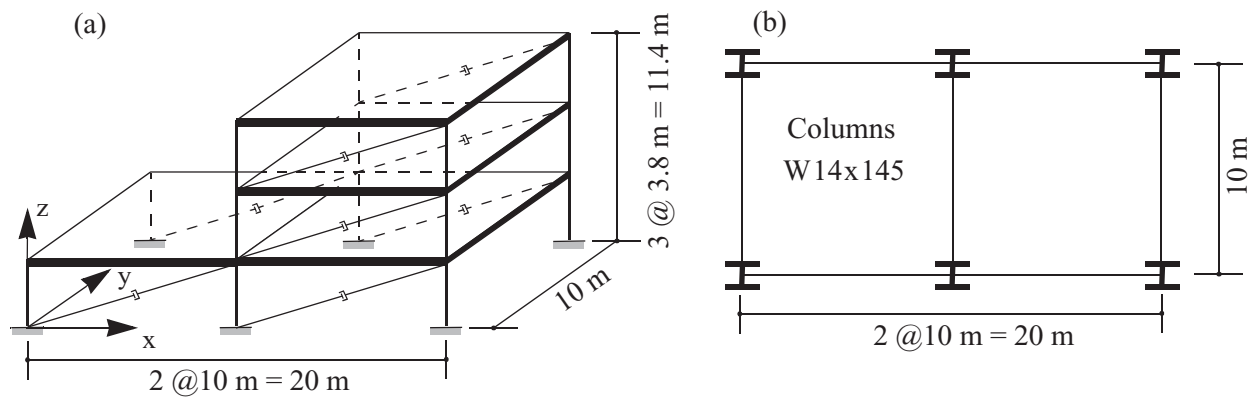
Accepted Manuscript
Not Copyedited

Figure 8

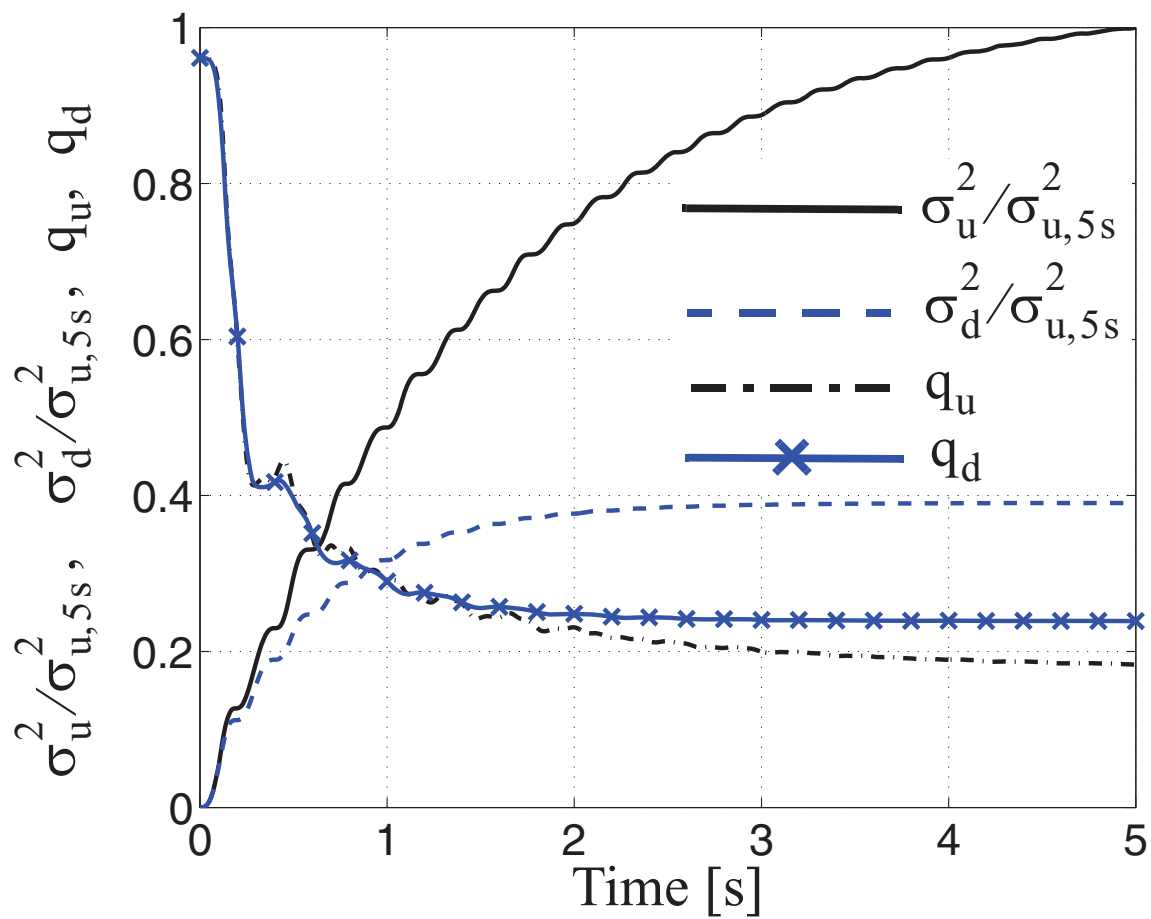
Journal of Engineering Mechanics. Submitted August 22, 2009; accepted November 16, 2010;
posted ahead of print November 18, 2010. doi:10.1061/(ASCE)EM.1943-7889.0000238



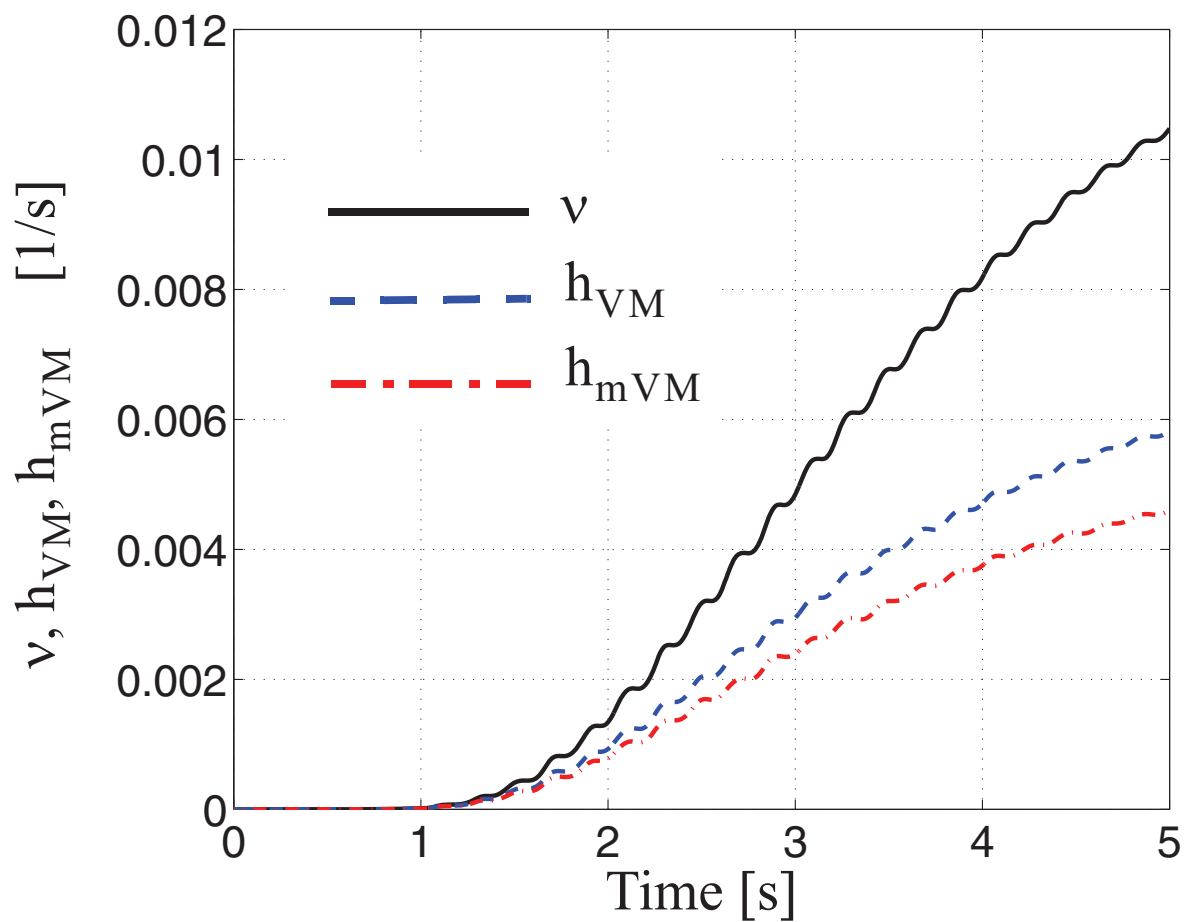
Accepted Manuscript
Not Copyedited



Accepted Manuscript
 Not Copyedited



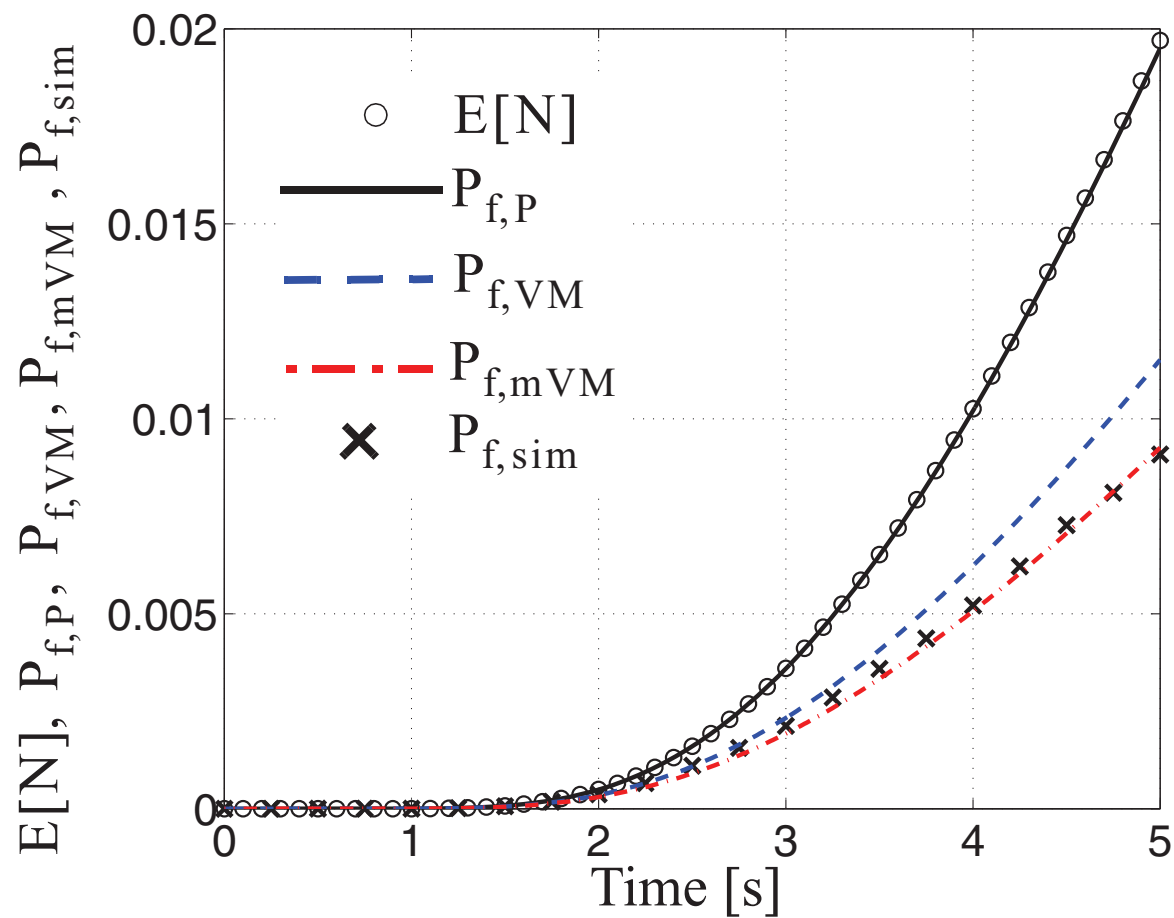
Accepted Manuscript
 Not Copyedited



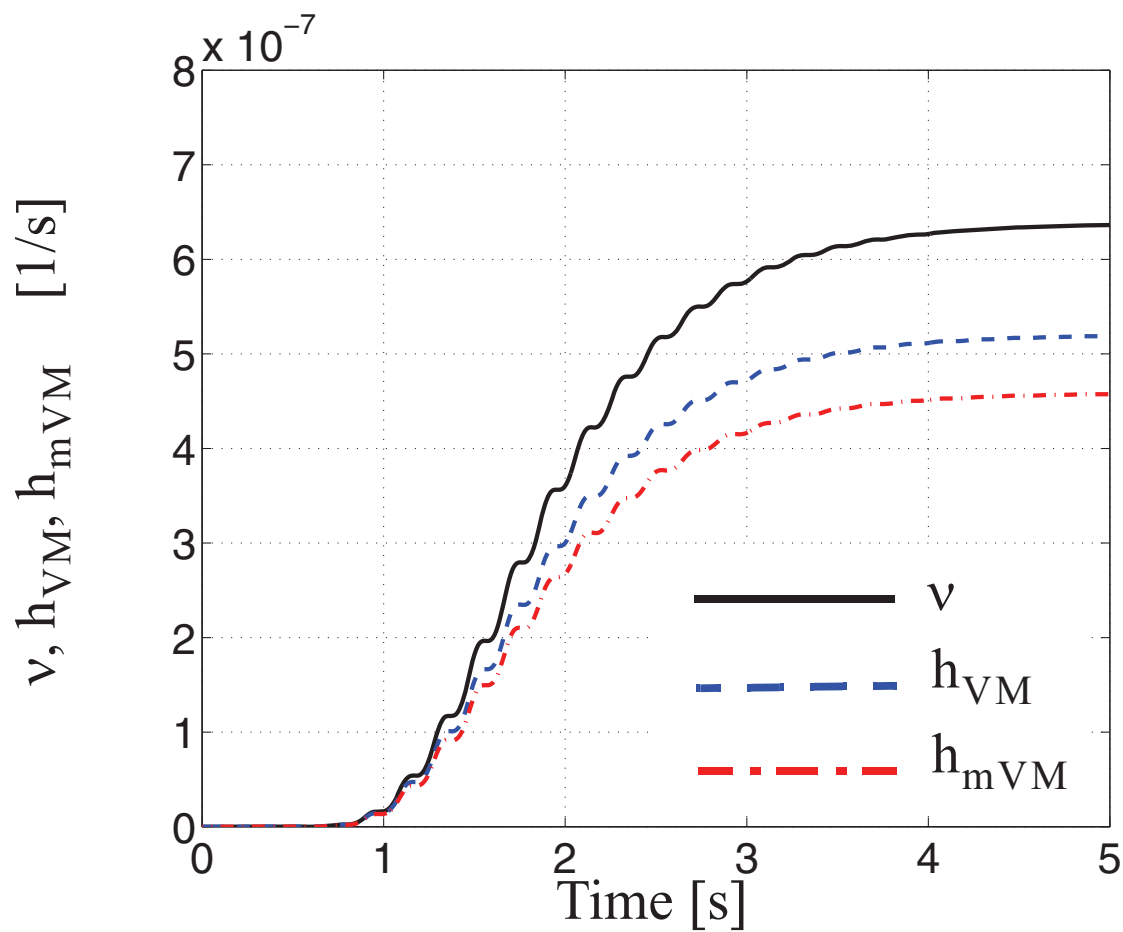
Accepted Manuscript
Not Copyedited

Figure 12

Journal of Engineering Mechanics. Submitted August 22, 2009; accepted November 16, 2010;
posted ahead of print November 18, 2010. doi:10.1061/(ASCE)EM.1943-7889.0000238

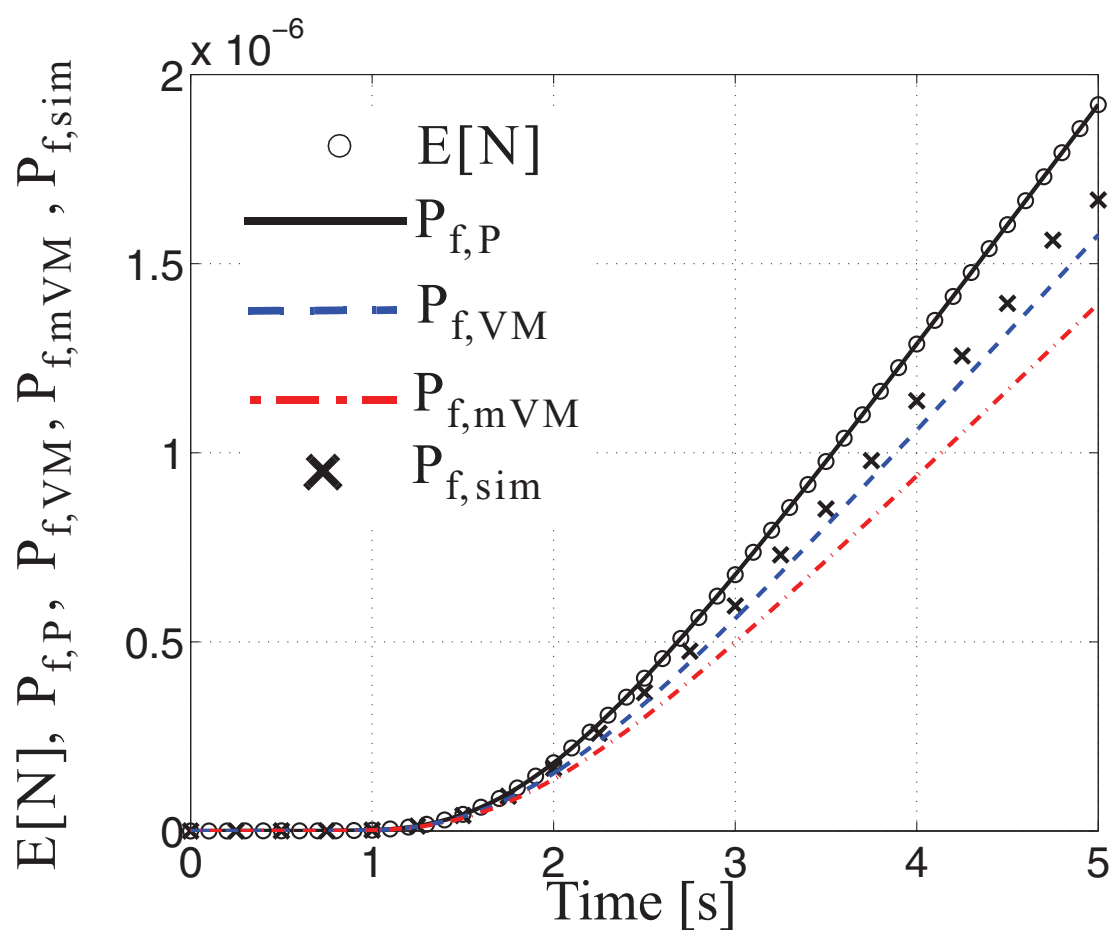


Accepted Manuscript
Not Copyedited

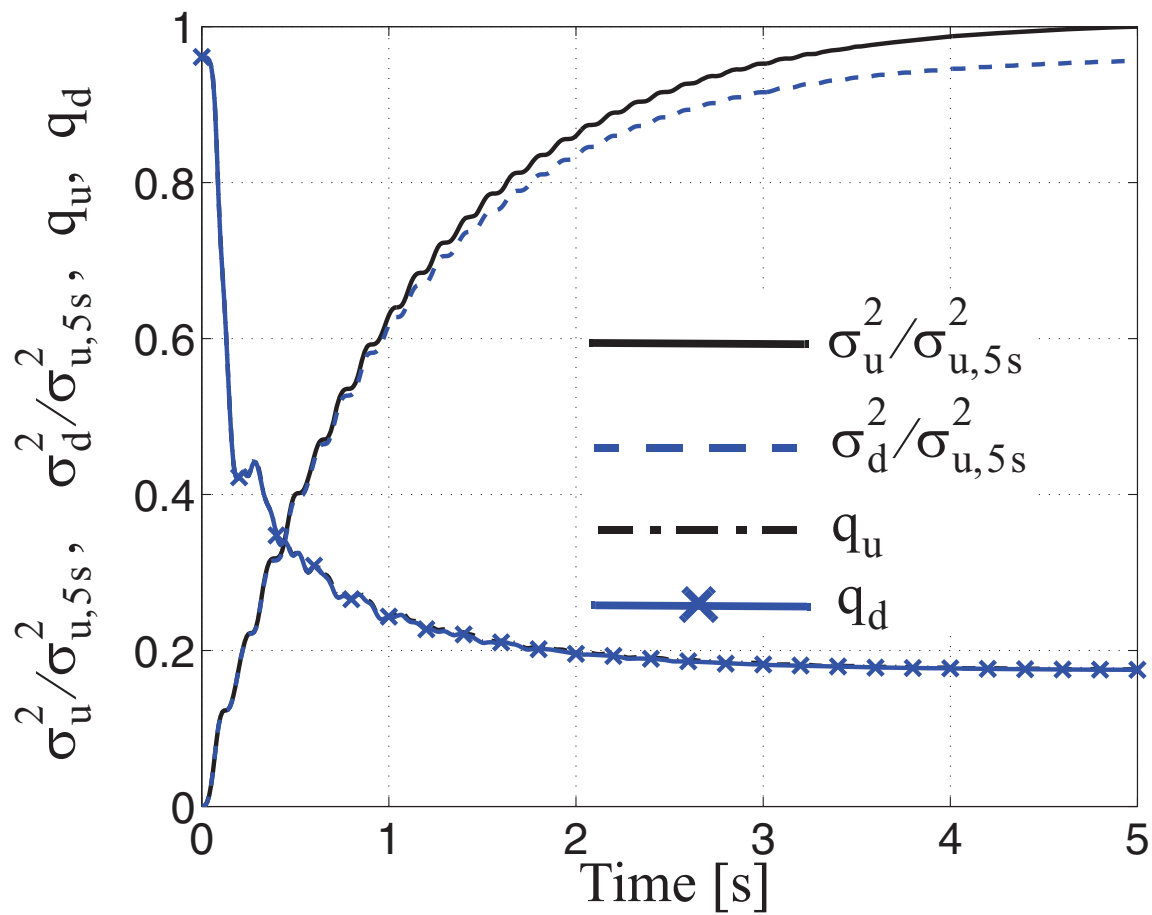


Accepted Manuscript
Not Copyedited

Figure 14



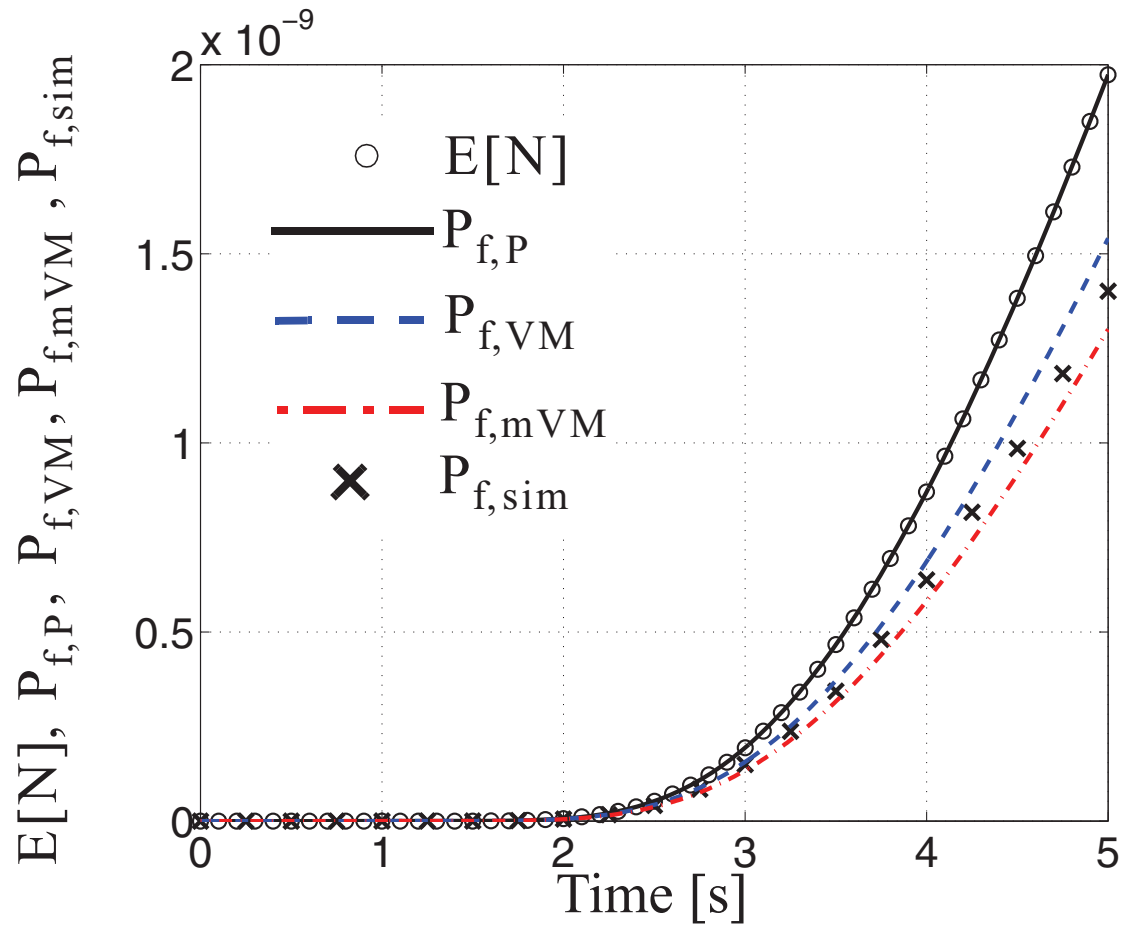
Accepted Manuscript
Not Copyedited



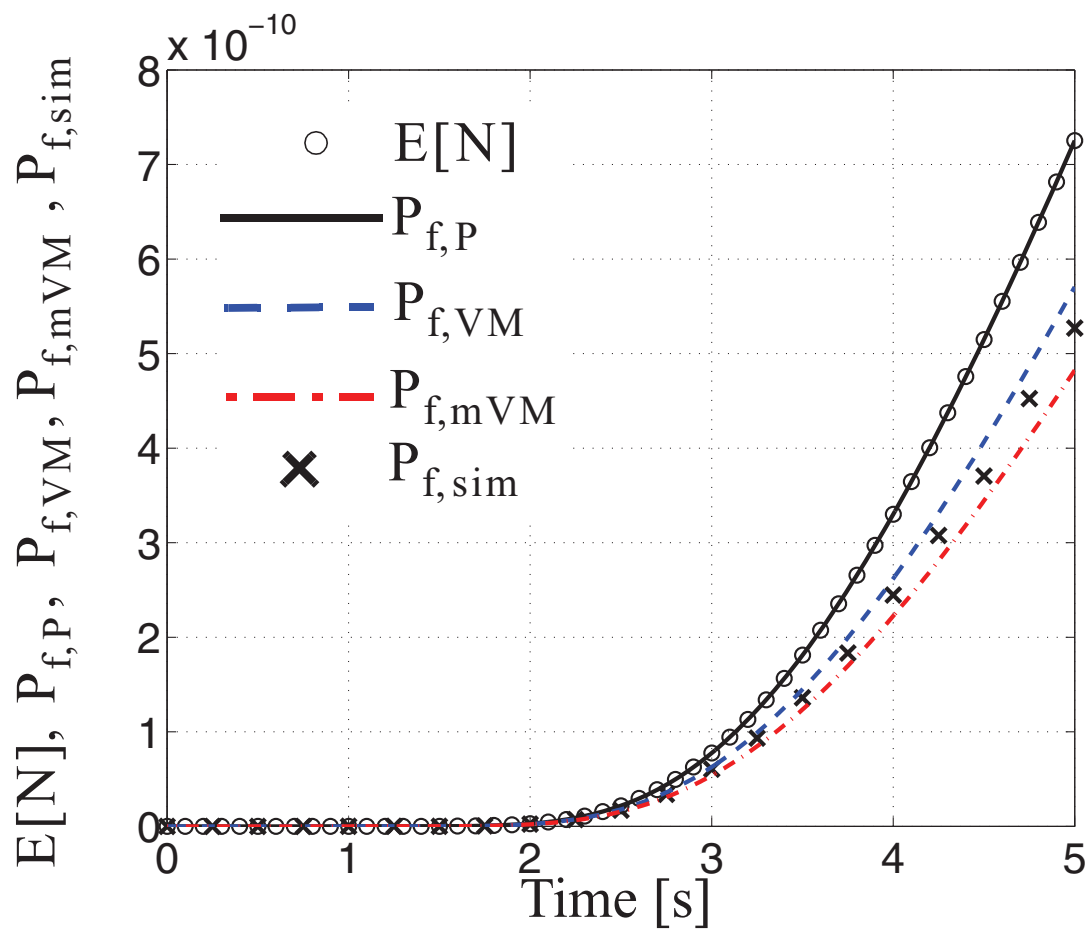
Accepted Manuscript
 Not Copyedited

Figure 16

Journal of Engineering Mechanics. Submitted August 22, 2009; accepted November 16, 2010;
posted ahead of print November 18, 2010. doi:10.1061/(ASCE)EM.1943-7889.0000238

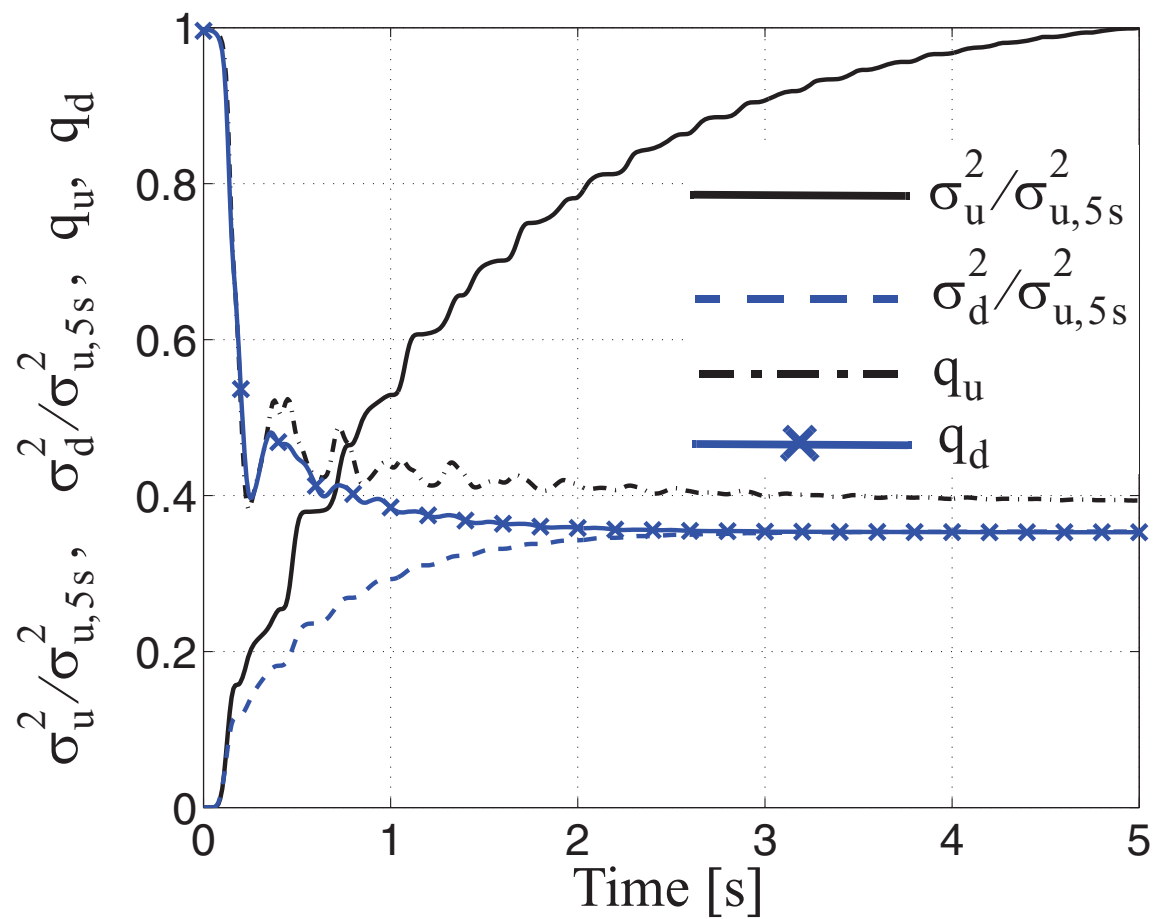


Accepted Manuscript
Not Copyedited

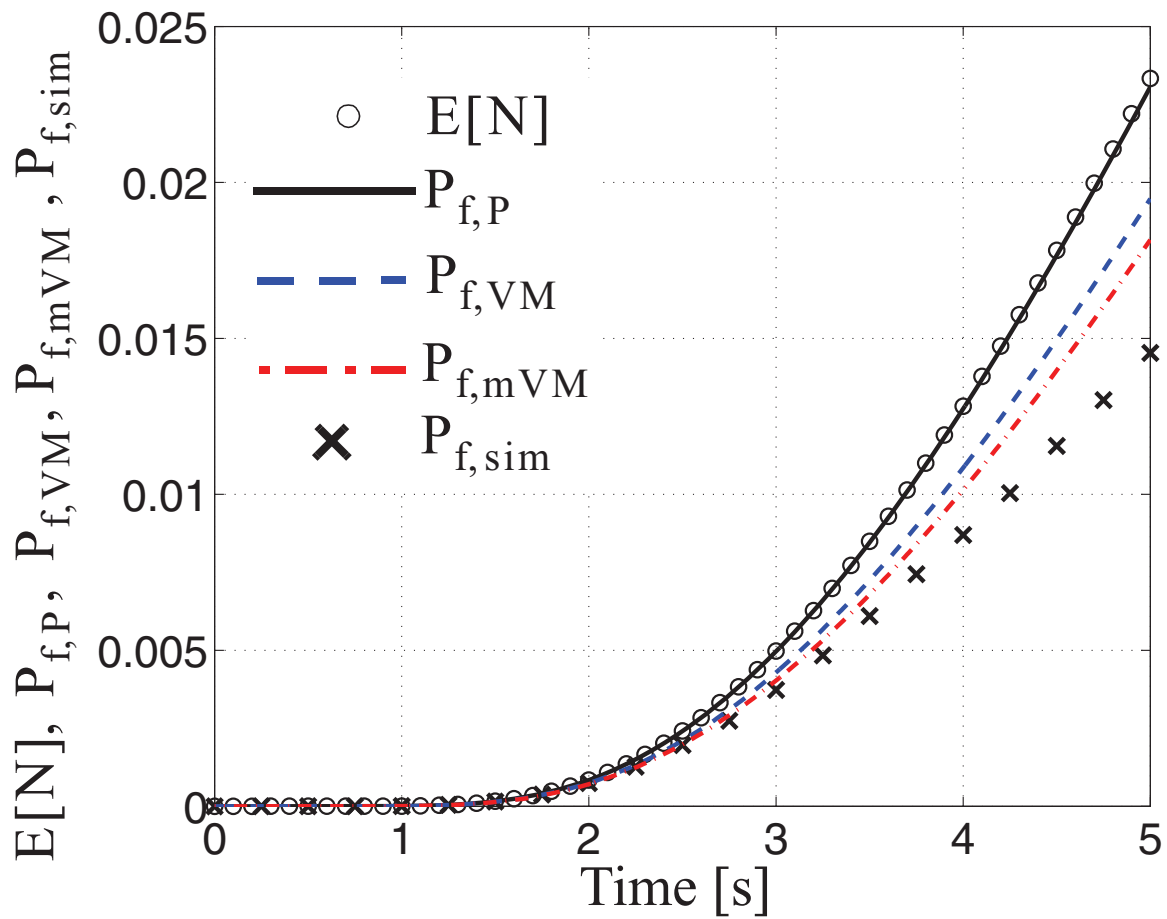


Accepted Manuscript
 Not Copyedited

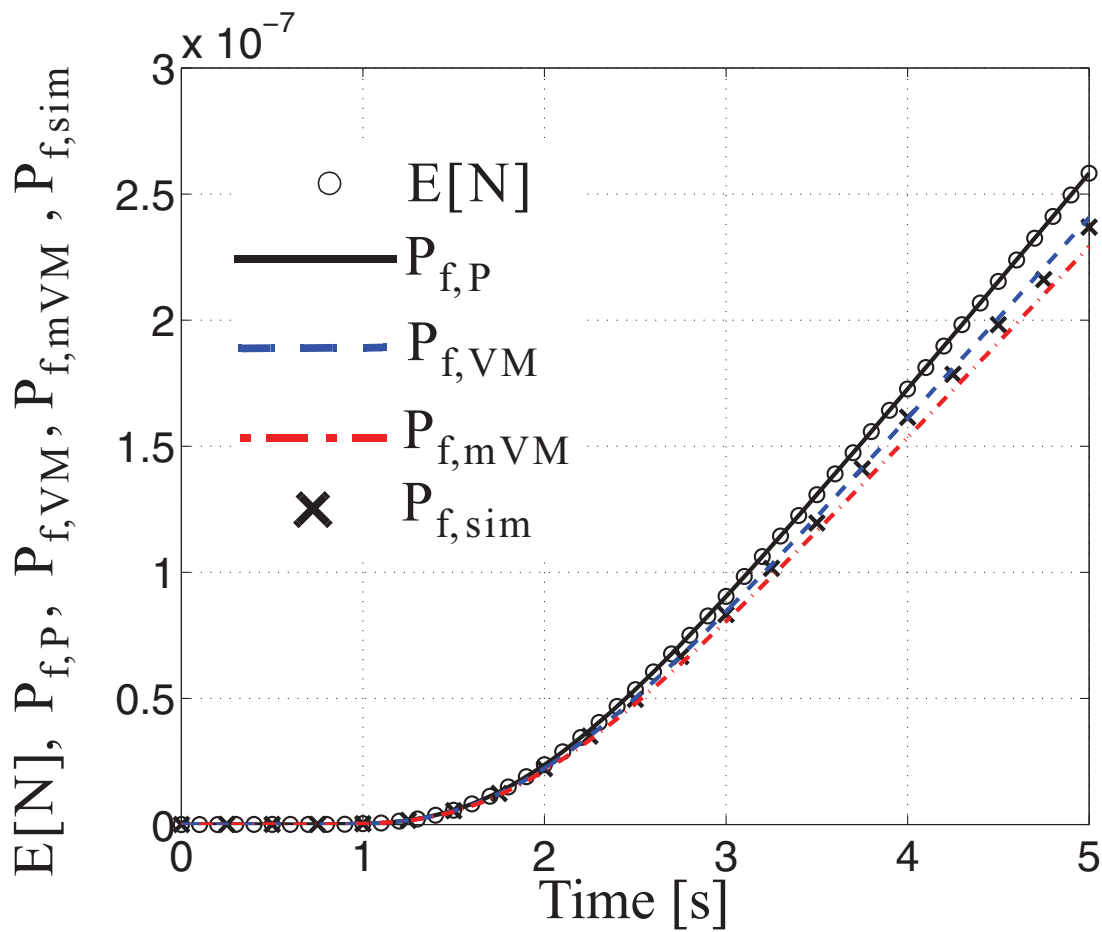
Figure 18



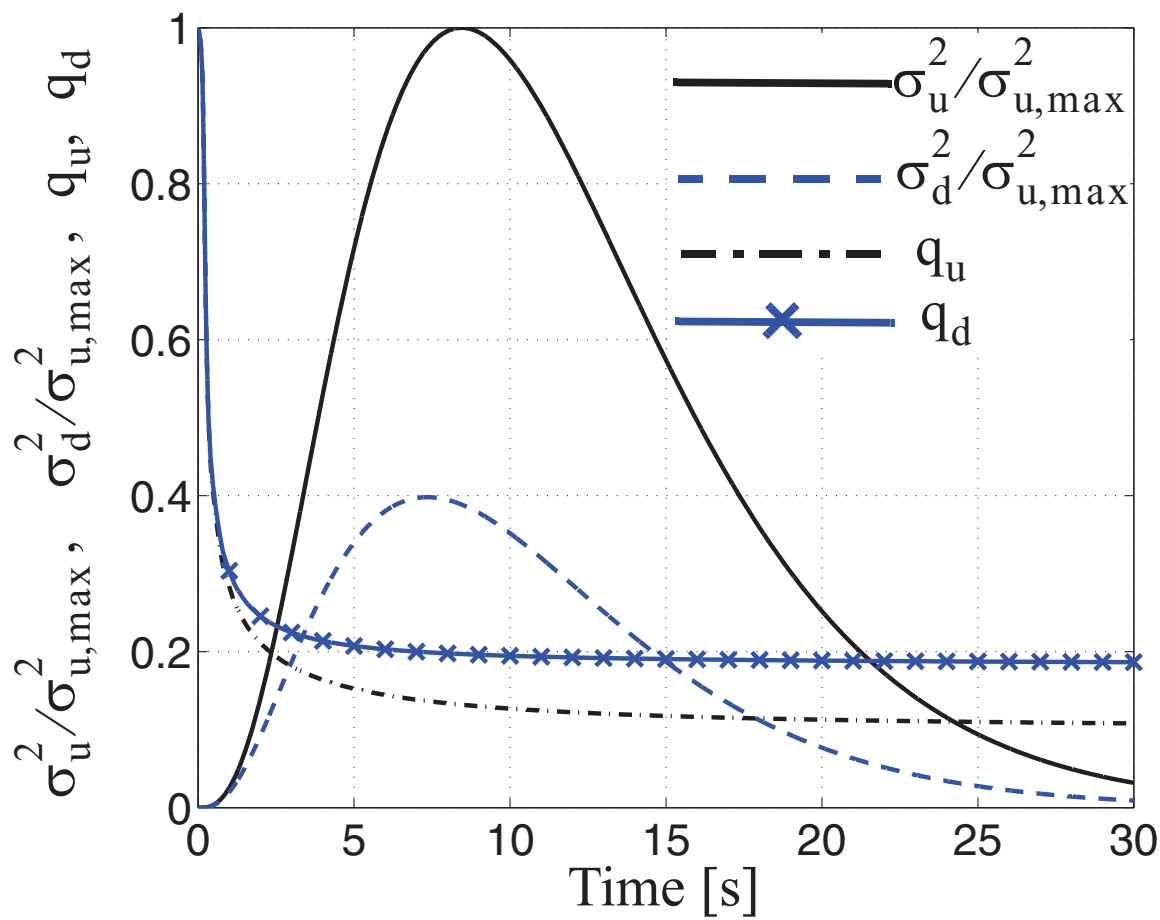
Accepted Manuscript
Not Copyedited



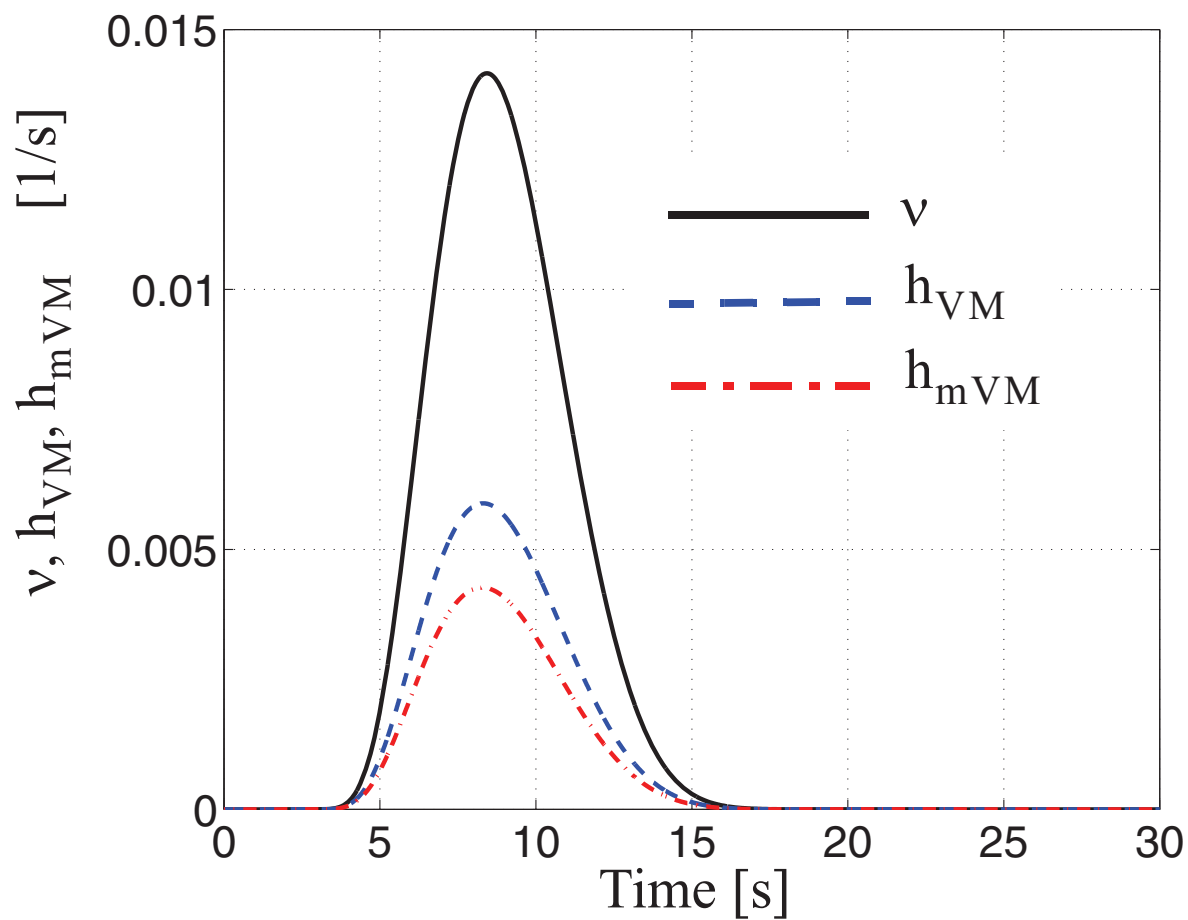
Accepted Manuscript
 Not Copyedited



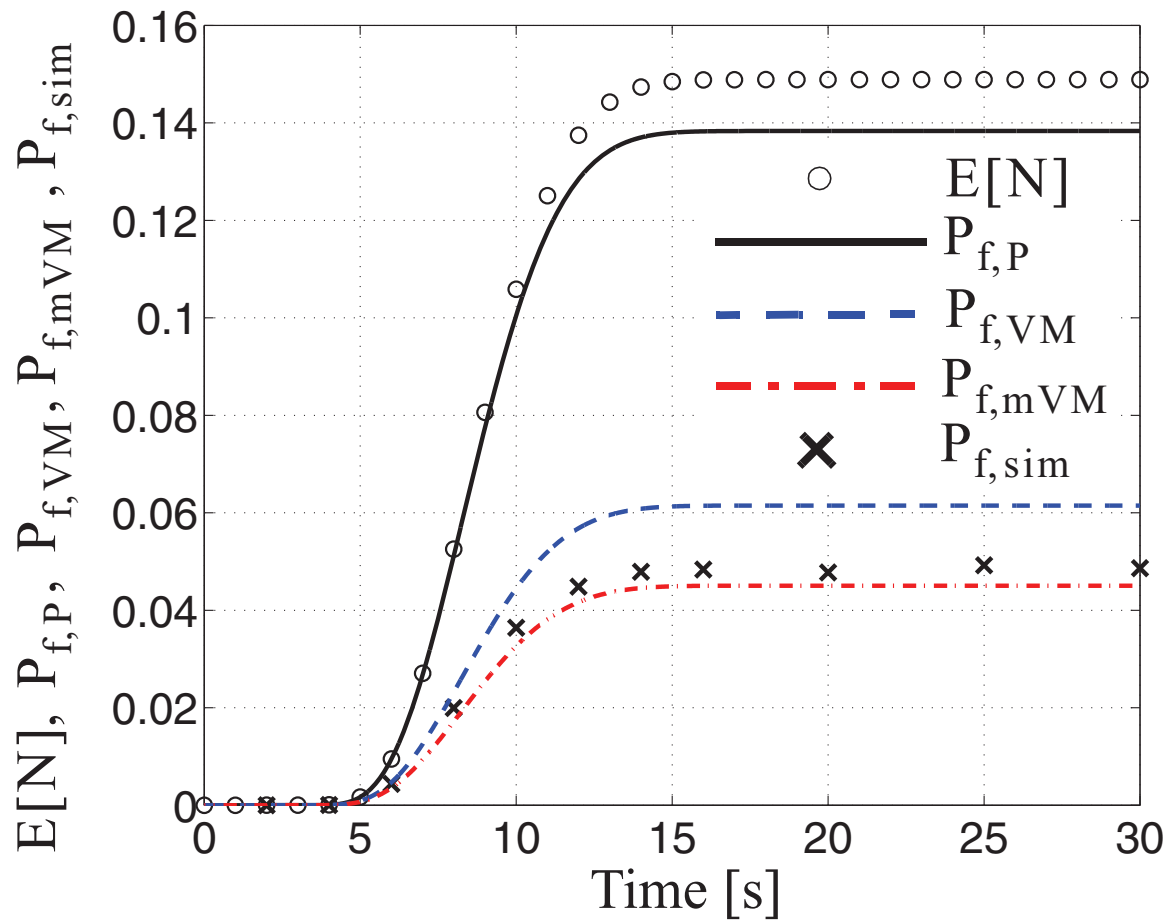
Accepted Manuscript
 Not Copyedited



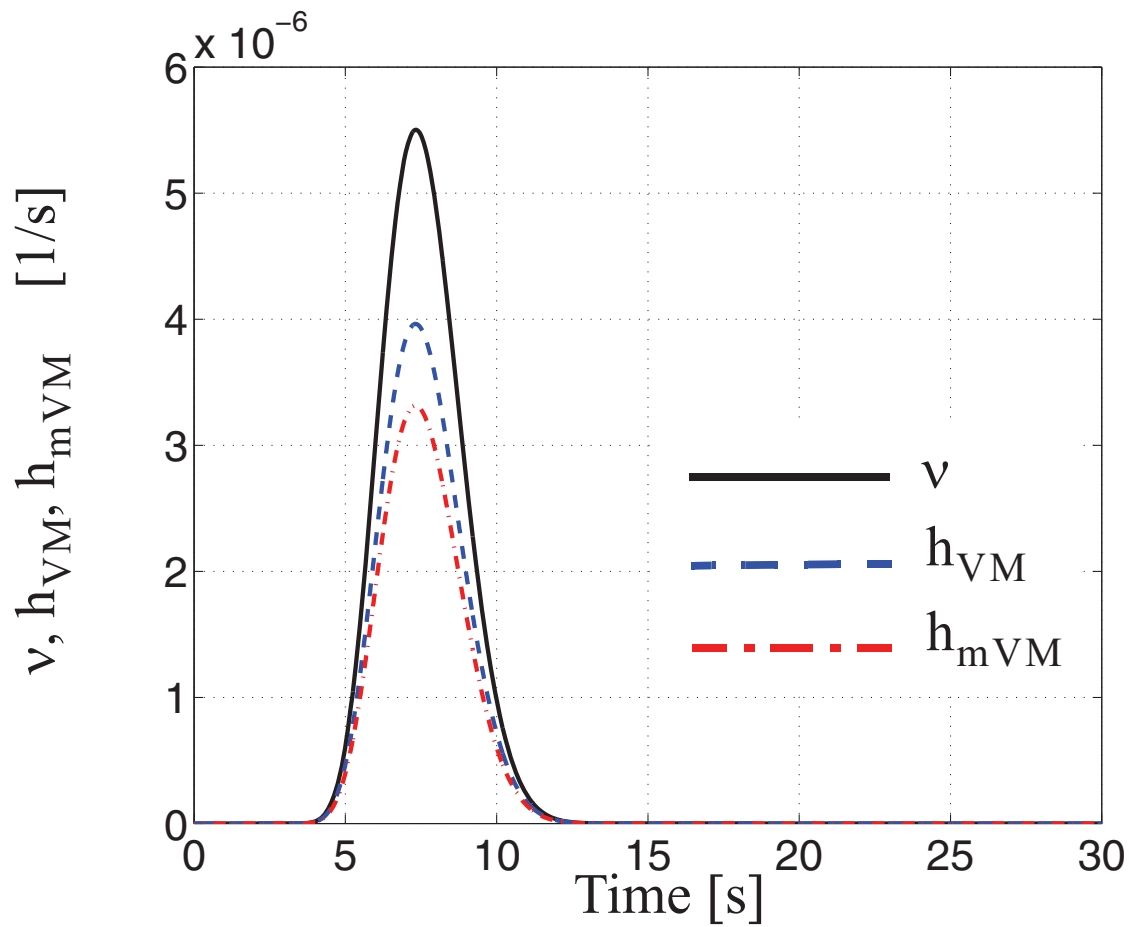
Accepted Manuscript
 Not Copyedited



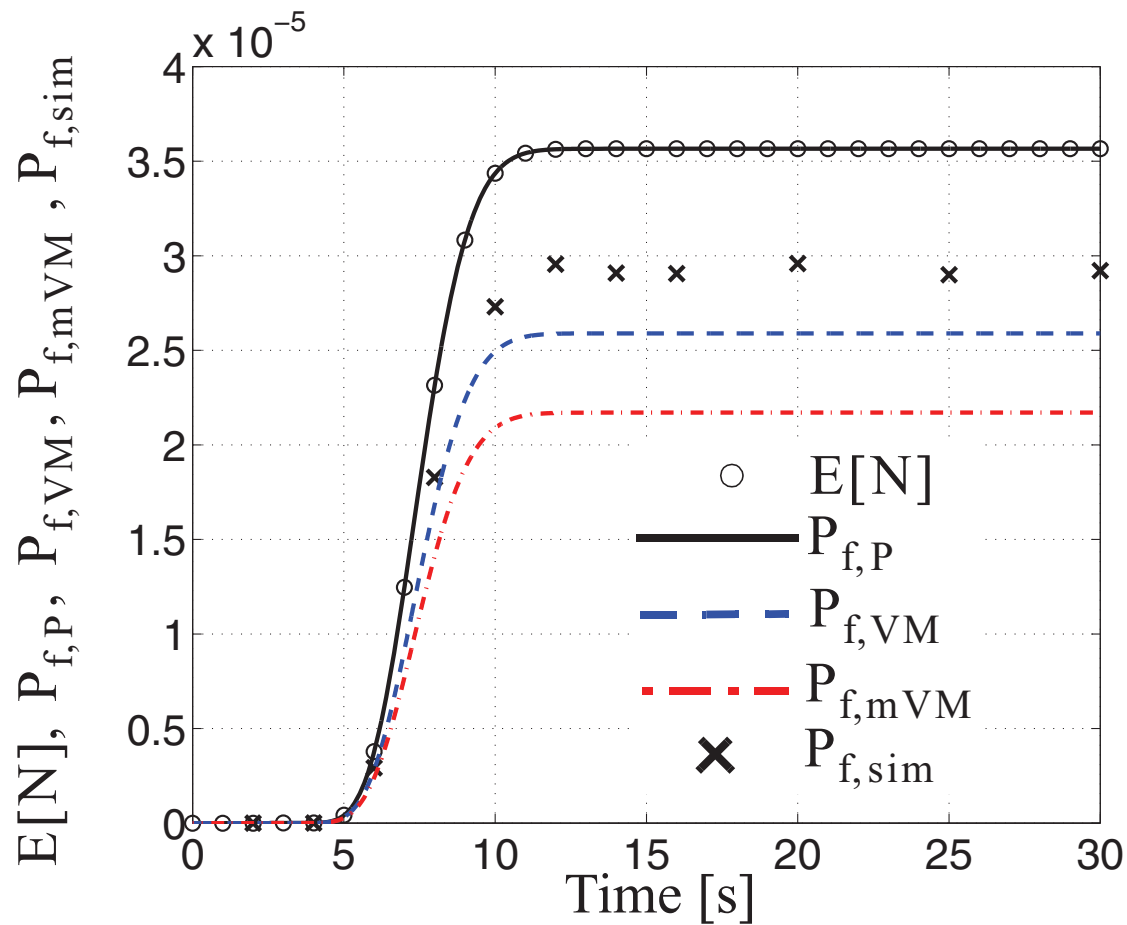
Accepted Manuscript
Not Copyedited



Accepted Manuscript
 Not Copyedited



Accepted Manuscript
Not Copyedited



Accepted Manuscript
 Not Copyedited

Table 1: Time-variant failure probability for linear elastic SDOF system with natural period $T_0 = 0.5\text{s}$
subjected to white noise base excitation from at rest initial conditions

Damping ratio ξ	Estimates	$\zeta = 2.0 \sigma_{U\infty}$		$\zeta = 3.0 \sigma_{U\infty}$		$\zeta = 4.0 \sigma_{U\infty}$	
		$t = 5T_0$	$t = 10T_0$	$t = 5T_0$	$t = 10T_0$	$t = 5T_0$	$t = 10T_0$
1%	P	0.030	0.339	8.1e-5	7.7e-3	2.9e-8	3.8e-5
	VM	0.018	0.166	5.7e-5	4.1e-3	2.3e-8	2.4e-5
	mVM	0.015	0.129	4.8e-5	3.1e-3	2.0e-8	1.9e-5
	ISEE	0.016	0.123	5.5e-5	3.3e-3	2.5e-8	2.2e-5
5%	P	0.507	0.868	0.038	0.134	7.7e-4	3.8e-3
	VM	0.346	0.678	0.026	0.087	5.8e-4	2.7e-3
	mVM	0.301	0.607	0.022	0.074	5.1e-4	2.4e-3
	ISEE	0.323	0.601	0.025	0.076	6.1e-4	2.7e-3
10%	P	0.641	0.907	0.070	0.168	1.9e-3	5.3e-3
	VM	0.506	0.798	0.053	0.126	1.6e-3	4.3e-3
	mVM	0.462	0.752	0.048	0.114	1.5e-3	3.9e-3
	ISEE	0.521	0.801	0.054	0.122	1.7e-3	4.6e-3

Accepted Manuscript
Not Copyedited

Table 2: Undamped natural frequencies and description of vibration mode shapes of the three-dimensional asymmetric building example

Mode #	ω_i [rad/s]	T_i [s]	Mode Shape Description
1	15.97	0.393	x-translation
2	24.12	0.261	y-translation + torsion
3	36.56	0.172	x-translation
4	41.21	0.153	y-translation + torsion
5	56.74	0.111	y-translation + torsion
6	56.98	0.110	x-translation
7	73.88	0.085	y-translation + torsion
8	95.15	0.066	y-translation + torsion
9	127.69	0.049	y-translation + torsion

Accepted Manuscript
 Not Copyedited